REPORT DOCUMENTATION PAGE

Form Approved
OMB No. 0704-0188

1. REPORT DATE
07 May 2018

2. REPORT TYPE
Conference Paper with Briefing Charts

3. DATES COVERED *(From - To)*
01 May 2018 - 01 February 2019

4. TITLE AND SUBTITLE
Evaluation of Multi-Phase Equations of State for Liquid Rocket Engine Combustion Modeling (Conference Paper with Briefing Charts)

5a. CONTRACT NUMBER

5b. GRANT NUMBER

5c. PROGRAM ELEMENT NUMBER

6. AUTHOR(S)
Harvazinski, M., Talley, D.

5d. PROJECT NUMBER

5e. TASK NUMBER

5f. WORK UNIT NUMBER
Q1RY

7. PERFORMING ORGANIZATION NAME(S) AND ADDRESS(ES)
Air Force Research Laboratory (AFMC)
AFRL/RQRC
10 E. Saturn Blvd.
Edwards AFB, CA 93524-7680

8. PERFORMING ORGANIZATION REPORT NUMBER

9. SPONSORING/MONITORING AGENCY NAME(S) AND ADDRESS(ES)

Air Force Research Laboratory (AFMC)
AFRL/RQR
5 Pollux Drive
Edwards AFB, CA 93524-7048

10. SPONSOR/MONITOR'S ACRONYM(S)

11. SPONSOR/MONITOR'S REPORT NUMBER(S)
AFRL-RQ-ED-TP-2019-045

12. DISTRIBUTION/AVAILABILITY STATEMENT
Distribution Statement A: Approved for Public Release; Distribution is Unlimited. PA Clearance Number: 19064 Clearance Date: 01 February 2019.

13. SUPPLEMENTARY NOTES
For presentation at JANNAF; Long Beach, CA, USA; May 21, 2018 (Presented at May 2018 JANNAF as Distribution C package - now being re-released with no changes - as a Distribution A package).
The U.S. Government is joint author of the work and has the right to use, modify, reproduce, release, perform, display, or disclose the work.
Conference Paper with Briefing Charts

14. ABSTRACT
Liquid rocket engines often operate in regimes where ideal gas equations of state are not applicable or have unacceptable levels of error. Mass flow rates are typically specified for the inlet boundary condition; without an appropriate value of the density the incoming fluid velocity will be incorrect. The error in density between an ideal gas and the actual value can be more than an order of magnitude under the high pressure low temperature conditions found some kinds of liquid rocket engine injectors. The use of cubic equations of state will provide better estimates of the density but can lead to additional challenges when the mixture is sub-critical and inside the vapor dome. The present work looks at the development of a multi-fluid model using a cubic equation of state. At a computational cell level the mixture is assumed to be homogeneous. To achieve this Amagats law of partial volumes is applied to generate mixture averaged thermodynamic properties including density and enthalpy. Amagats law of partial volumes is applicable to mixtures of real gases unlike Daltons law of partial pressures which is only applicable to mixtures of ideal gases.

15. SUBJECT TERMS
N/A

16. SECURITY CLASSIFICATION OF:			**17. LIMITATION OF ABSTRACT**	**18. NUMBER OF PAGES**	**19a. NAME OF RESPONSIBLE PERSON**
					D. Talley
a. REPORT	**b. ABSTRACT**	**c. THIS PAGE**			**19b. TELEPHONE NUMBER** *(Include area code)*
Unclassified	Unclassified	Unclassified	SAR	52	N/A

EVALUATION OF MULTI-PHASE EQUATIONS OF STATE FOR LIQUID ROCKET ENGINE COMBUSTION MODELING

M.E. Harvazinski and D.G. Talley
AFRL Rocket Lab
Edwards AFB, CA

ABSTRACT

Liquid rocket engines often operate in regimes where ideal gas equations of state are not applicable or have unacceptable levels of error. Mass flow rates are typically specified for the inlet boundary condition; without an appropriate value of the density the incoming fluid velocity will be incorrect. The error in density between an ideal gas and the actual value can be more than an order of magnitude under the high pressure low temperature conditions found some kinds of liquid rocket engine injectors. The use of cubic equations of state will provide better estimates of the density but can lead to additional challenges when the mixture is sub-critical and inside the vapor dome. The present work looks at the development of a multi-fluid model using a cubic equation of state. At a computational cell level the mixture is assumed to be homogeneous. To achieve this Amagats law of partial volumes is applied to generate mixture averaged thermodynamic properties including density and enthalpy. Amagats law of partial volumes is applicable to mixtures of real gases unlike Daltons law of partial pressures which is only applicable to mixtures of ideal gases.

INTRODUCTION

Liquid rocket engines can operate at pressures exceeding 100 atm in full size engines and preburners. While the propellants are typically injected at supercritical pressures their temperature can be subcritical. This presents a modeling challenge in accurately capturing their thermodynamic properties. The complexity worsens because the propellants are injected into a mixture environment comprised of reactants and products. The supercritical state of a mixture is a function of not only the temperature and pressure but also the composition. When species with very large critical pressures like carbon dioxide or water are present the mixture can become subcritical, even for small amounts of these species. The presence of water and carbon dioxide as combustion products will be present as combustion takes place. The subcritical and supercritical regions of the flow will have thermodynamic and transport properties that are dramatically different from each other. These lead to gradients in the flowfield that will influence mixing and in turn the dynamics in the combustor. After complete combustion has taken place the temperature is high enough that the problem is alleviated. Computational modeling of this transitional state is challenging and is the subject of the current work.

Distribution Statement A: Approved for public release; distribution is unlimited. PA Clearance Number 19xxx

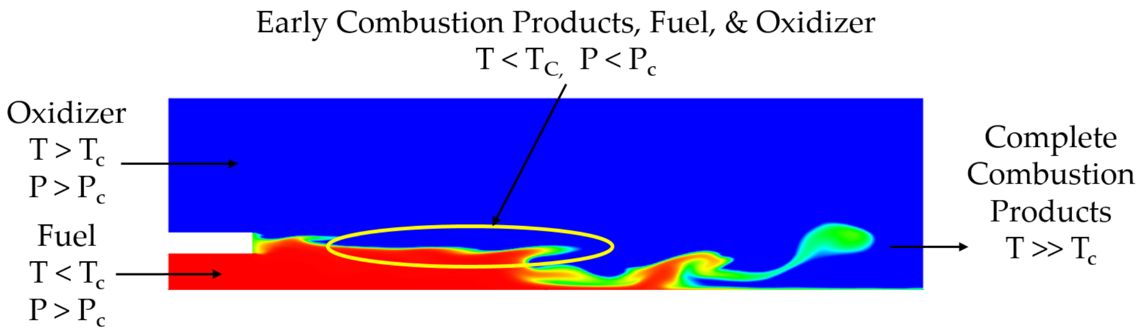

Figure 1: Shear layer schematic showing the different regions of the flow. In a typical rocket injector the oxidizer is injected at a temperature that is above the critical temperature and pressure, the fuel is injected at a temperature less than the critical temperature but a pressure above the critical pressure. Complete combustion products have a temperature much larger than the critical temperature. The challenging region is the early combustion products region where both the temperature and pressure can be sub-critical.

The current approach is to simulate the liquid-like fluid as a dense gas, with the properties provided by a real gas equation of state. The applicability of these non-ideal equations of state is not completely understood at this time. Numerical instabilities are frequently present in computations which utilize a cubic equation of state. Other more sophisticated equations of state like the Benedict Webb Rubin offer a wider range of applicability but the cost associated with them are intractable for large 3D LES simulations [?]. Other modeling approaches are also possible but they are much more involved and also involve significant cost increases. Models like a volume of fluid approach (VOF) for instance would be extremely costly for a large simulation because of the interface tracking required. Other more empirically based models for atomization can also be used in some situations.

A substantial amount of experimental work has been directed at studying the behavior of jets in transcritical environments in recent years. Chehroudi et al. collected visual images along with jet spreading rates for jet injection into like and unlike ambient fluids for both subcritical and supercritical conditions [?, ?]. Roy et al. performed experimental work on the injection of supercritical jets into subcritical environments. Results showed a variety of regimes depending on the mixture. This indicates that this is an extremely complex operating state without clearly defined flow regimes [?]. Modeling work has been led by Okong'o et al. and has primarily focused on a supercritical binary mixing in a mixing layer configuration using DNS [?]. Further work by Masi et al. on turbulent mixing layers developed effective locally varying turbulent Schmidt and Prandtl numbers which were observed to have negative values [?].

In a comprehensive review article, Bellan stated that a real gas equation of state along with unsteady simulations are the absolute minimum requirements for capturing supercritical behavior [?]. Oefelein simulated combustion between transcritical oxygen and supercritical hydrogen. It was found that intense property gradients were present that approached contact discontinuities which can be difficult to model [?]. Recently, Dahms and Oefelein have proposed a theoretical framework for assessing when a propellant mixture behaves as a supercritical dense fluid and when transcritical phenomena needs to be considered [?]. To date most modeling has focused on purely supercritical environments.

This work presents an overview of the Peng-Robinson Equation of state and several of the challenges associated with using it to simulate liquid rocket injector configurations. Several alternate approaches are presented as possible paths forward in applying real gas equations of state to liquid rocket injectors. Demonstration cases are used to show some of the effects that these alternate approaches have. The motivation for this work is liquid rocket injector simulations, Figure 1 shows a schematic of a liquid rocket injector shear layer. Different regions of the flowfield are shown. In a typical rocket injector the oxidizer is injected at a temperature that is above the critical temperature and pressure, the fuel is injected at a temperature less than the critical temperature but a pressure above the critical pressure. Complete combustion products have a temperature much larger than the critical temperature and in this region the challenges are no longer present. The challenging region is the early combustion products region where both the temperature and pressure can be sub-critical.

PENG ROBINSON EQUATION OF STATE

The Peng Robinson equation of state [**?**] is a cubic equation of state that can be written as,

$$p = \frac{RT}{V_m - b_m} - \frac{a_m}{V_m^2 + 2b_m V_m - b_m^2} \tag{1}$$

It is only one of several possible cubic equations of state. A comprehensive overview of other equations of state is given by Poling et al. [**?**]. In the case of multiple species the parameters a_m and b_m are defined in terms of a series of mixing rules,

$$a_m = \sum_{j=1}^{N} \sum_{i=1}^{N} X_i X_j \sqrt{a_i a_j} k'_{ij} \tag{2}$$

$$b_m = \sum_{i=1}^{N} X_i b_i \tag{3}$$

The parameter k'_{ij} is an interaction index and is typically unity unless otherwise specified for a pair of species. The individual parameters a_i and b_i correspond to the single species values which are defined as,

$$a_i = 0.457235 \frac{R^2 T_{c,i}^2}{p_{c,i}} \left(1 + \kappa_i (1 - \sqrt{T_r})\right)^2 \tag{4}$$

$$b_i = 0.077796 \frac{R T_{c,i}}{p_{c,i}} \tag{5}$$

The parameter κ_i is defined in terms of the acentric factor ω_i,

$$\kappa_i = 0.37464 + 1.54226\omega_i - 0.26992\omega_i^2 \tag{6}$$

In addition to the acentric factor the critical pressure $p_{c,i}$ and the critical temperature $T_{c,i}$ are constants of the individual species. The motivation for using the cubic equation of state is to determine the deviation from the ideal behavior. For density the non-ideal behavior is determined through the compressibility Z, which is the roots to the equation,

$$Z^3 - (1 - B)Z^2 + (A - 2B - 3B^2)Z - (AB - B^2 - B^3) = 0 \tag{7}$$

The parameters A and B depend on the mixture and are related to a_m and b_m,

$$A = a_m \frac{p}{R^2 T^2} \tag{8}$$

$$B = b_m \frac{p}{RT} \tag{9}$$

Once the compressibility is known it is possible to compute the real gas density,

$$\rho = \frac{pW}{ZRT} \tag{10}$$

Where W is the molecular weight of the mixture,

$$W = \left(\sum_{i=1}^{N} \frac{Y_i}{W_i} \right)^{-1} \tag{11}$$

Other thermodynamic quantities are related to their corresponding ideal gas quantity using a departure function. For a typical reacting flow simulation the specific heat, enthalpy and Gibbs energy are needed. The departure functions for these three quantities are,

$$c^{\mathrm{dep}} = \left.\frac{\partial h^{\mathrm{dep}}}{\partial T}\right|_{p} \tag{12}$$

$$\frac{h^{\mathrm{dep}}}{RT} = (1 - Z) + \int_{V}^{\infty} T \left.\frac{\partial Z}{\partial T}\right|_{V} \frac{dV}{V} \tag{13}$$

$$\frac{g^{\mathrm{dep}}}{RT} = (1 - Z + \ln Z) + \int_{V}^{\infty} (1 - Z)\frac{dV}{V} \tag{14}$$

Most computational solvers do not work with molar volume so it is useful to carry out the integration using the Peng Robinson equation of state and convert to units native to the solver. Completing the integration yields,

$$c_p^{\mathrm{dep}} = \frac{1}{W}\left(R\left(T\frac{\partial Z}{\partial T} + Z - 1\right) - \frac{1}{\sqrt{8}b_m}\left[Ta_m'' \ln(\alpha) - (a_m - Ta_m')\, b^{\star}\beta\right]\right) \tag{15}$$

$$\frac{h^{\mathrm{dep}}}{RT} = \frac{1}{W}\left((Z - 1) + \frac{a_m - Ta_m'}{\sqrt{8}RTb_m}\ln\left\{\frac{Z/B + 1 - \sqrt{2}}{Z/B + 1 + \sqrt{2}}\right\}\right) \tag{16}$$

$$\frac{g^{\mathrm{dep}}}{RT} = \frac{1}{W}\left(Z - \ln(Z - B) - 1 + \frac{a_m}{\sqrt{8}RTb_m}\ln\left\{\frac{Z/B + 1 - \sqrt{2}}{Z/B + 1 + \sqrt{2}}\right\}\right) \tag{17}$$

Where a_m' is the derivative of a_m with respect to temperature, a_m'' is the second derivative of a_m with respect to temperature. The parameters $b^{\star}$ and β are,

$$b^{\star} = \frac{1}{B}\left(\frac{\partial Z}{\partial T} - \frac{Z}{B}\frac{\partial B}{\partial T}\right) \tag{18}$$

$$\beta = \frac{1}{Z/B + 1 - \sqrt{2}} - \frac{1}{Z/B + 1 + \sqrt{2}} \tag{19}$$

The presence of the molecular weight on the right side of the equation yields massic departure functions. The real gas specific heat, enthalpy, and Gibbs energy are then,

$$c_p = c_p^{\mathrm{dep}} + \sum_{i=1}^{N} c_{p,i}^{\mathrm{ig}} \tag{20}$$

$$h = h^{\mathrm{dep}} + \sum_{i=1}^{N} h_i^{\mathrm{ig}} \tag{21}$$

$$g = g^{\mathrm{dep}} + \sum_{i=1}^{N} g_i^{\mathrm{ig}} \tag{22}$$

The ideal gas values are readily available from the polynomial fit data,

$$\frac{c_{p,i}^{\mathrm{ig}}}{R_i} = \frac{c_1}{T^2} + \frac{c_2}{T} + c_3 + c_4T + c_5T^2 + c_6T^3 + c_7T^4 \tag{23}$$

$$\frac{h_i^{\mathrm{ig}}}{R_i} = -\frac{c_1}{T} + c_2\ln T + c_3T + \frac{c_4}{2}T^2 + \frac{c_5}{3}T^3 + \frac{c_6}{4}T^4 + \frac{c_7}{5}T^5 + c_8 \tag{24}$$

$$\frac{g_i^{\mathrm{ig}}}{R_iT} = -\frac{c_1}{2T^2} + \frac{c_2(\ln T + 1)}{T} + c_3(1 - \ln T) - \frac{c_4}{2}T + -\frac{c_5}{6}T^2 + -\frac{c_6}{12}T^3 - \frac{c_7}{20}T^4 + \frac{c_8}{T} - c_9 \tag{25}$$

Where the nine values of c_i can be found tabulated for individual species over multiple temperature ranges. Using this formulation for a mixture of species yields a single compressibility and set of departure functions for the mixture which are a function of the local pressure, temperature, and composition.

CHALLENGES

ROOTS OF THE PENG ROBINSON EQUATION OF STATE

The non-linearity and complexity of the cubic equation of state introduces numerous challenges when applying this equation of state to numerical simulations. Before considering specific challenges it is useful to understand the roots of the compressibility and their physical meaning. The Peng Robinson equation of state is valid for both gases and liquids. Accuracy in the liquid regime is sometimes less than is required. In that case the accuracy can be improved though a volume shifting procedure [**?**]. The compressibility is a multi-valued function in that the solution to equation 7 has three roots. Only positive real roots are of physical interest. There are three possible cases, three unique real roots, a single positive real root, or repeated positive real roots. The case of interest is the case of multiple unique real root. Figure 2 shows how the compressibility varies for water at 2 MPa as the temperature increases from 200 K to 800 K. The challenge with this plot is the abrupt change that occurs in the region where multiple positive real roots exists. While the transition between Z_1, Z_2, and Z_3 is a smooth curve, the maximum value of Z is not a smooth curve, this can lead to abrupt property changes. In a mixture the situation is further complicated because the transition is a function of pressure, temperature and composition. Simulations done using the traditional Peng Robinson equation of state have suffered from instabilities which are expected to arise from this phenomena.

Recent work by Harvazinski et al. attempted to smooth the compressibility in this region to generate a unique solution as the flow transitions across the dome. While this worked well for density there were unwanted changes in other properties, specifically the specific heat and sound speed. These properties were extremely sensitive to the smoothing operation. Numerous types of smoothing were considered but all introduced unacceptable changes in one or more other thermodynamic quantities despite yielding a smooth density [**?**].

PROPERTY VARIATIONS

Around the critical point there is extreme variation in the thermodynamic properties. Figure 3 shows the prediction of the sound speed and specific heat of water at 2 MPa for H_2O. A log scale is required to capture the variation. Over the range of 200 K to 500 K, the specific heat has a maximum value of $16,000\,\mathrm{J/kg\cdot K}$ and a minimum value of $2,130\,\mathrm{J/kg\cdot K}$. The sound speed also shows significant variations. This is problematic because the flow can become locally supersonic as the sound speed drops to a very small value. Figure 4 shows the sound speed in a reacting shear layer computed with the Peng Robinson equation of state. The sound speed on either side of the shear layer differs by an order of magnitude. The property variations and associated gradients in the flowfield give rise to a numerical problem that is not well posed in all situations. This can lead to divergent solutions and other numerical instabilities. The motivation for the following section is to devise alternate equations of state based on the Peng Robinson equation of state which yield the properties needed but hopefully eliminate some of the unwanted numerical effects.

ALTERNATIVE FORMULATIONS

DALTON'S LAW AND AMAGAT'S LAW

Typically mixing rules can be based off of either Dalton's law of partial pressures or Amagat's law of partial volumes. Dalton's law of partial pressures states that,

$$p = \sum_{i=1}^{N} p_i \tag{26}$$

where p_i is the partial pressure of species i. To compare each of these mixing rules with the traditional Peng Robinson equation of state, the mixture compressibility is compared. Define Z_i to

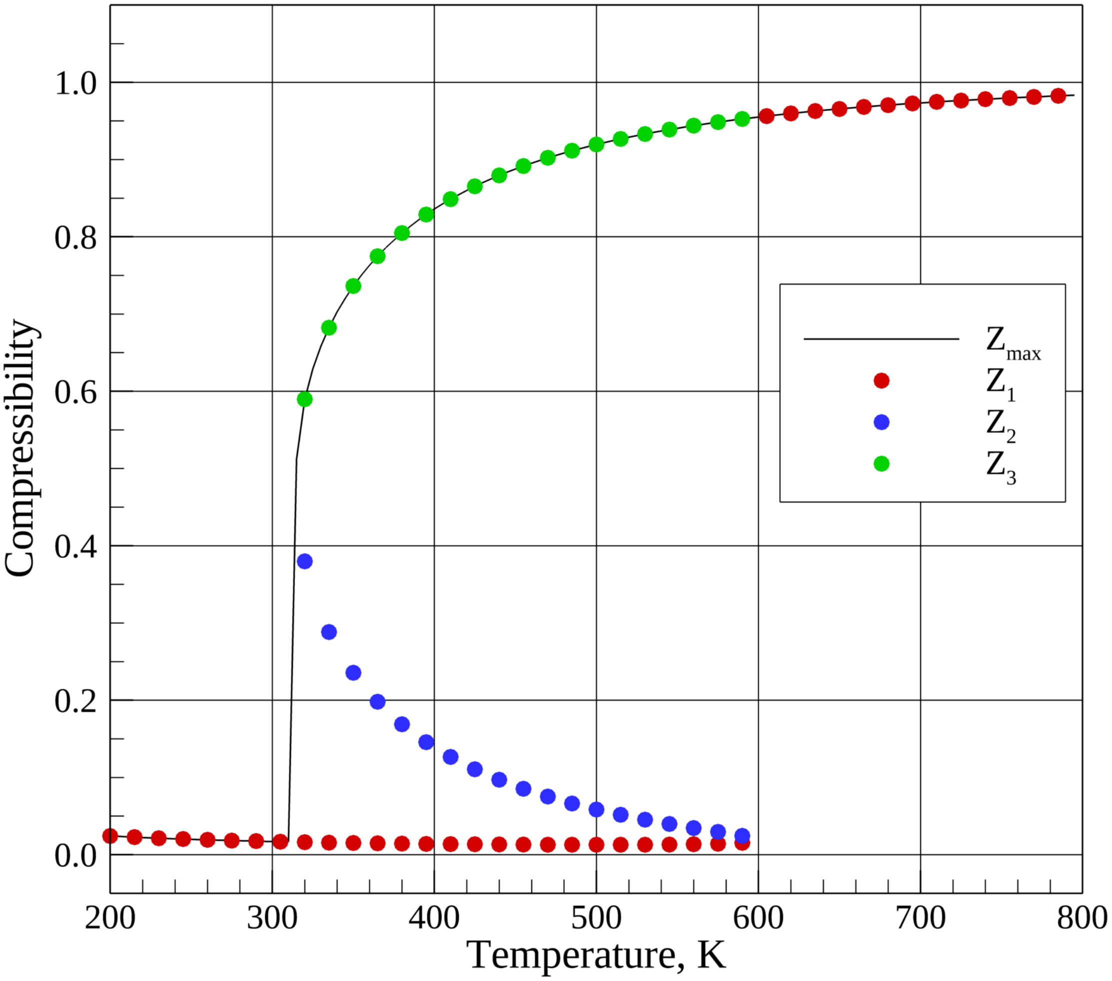

Figure 2: Root of equation 7 are shown as symbols as the temperatre is increased. The substance shown is water at 2 MPa. The solid line is the maxium compressibility which is used in the computation of the density and departure functions.

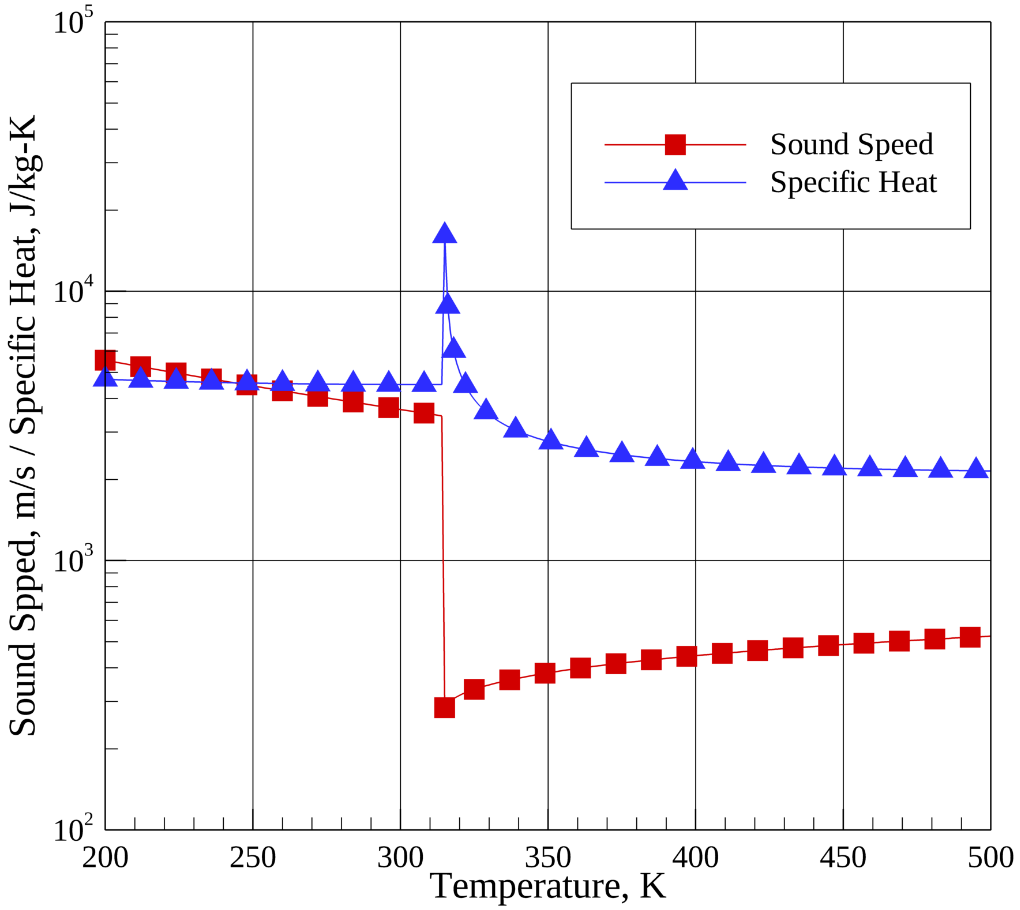

Figure 3: Sound speed and speicifc heat variations for H_2O at 2 MPa. The sound speed and specific heat are plotted on a log scale.

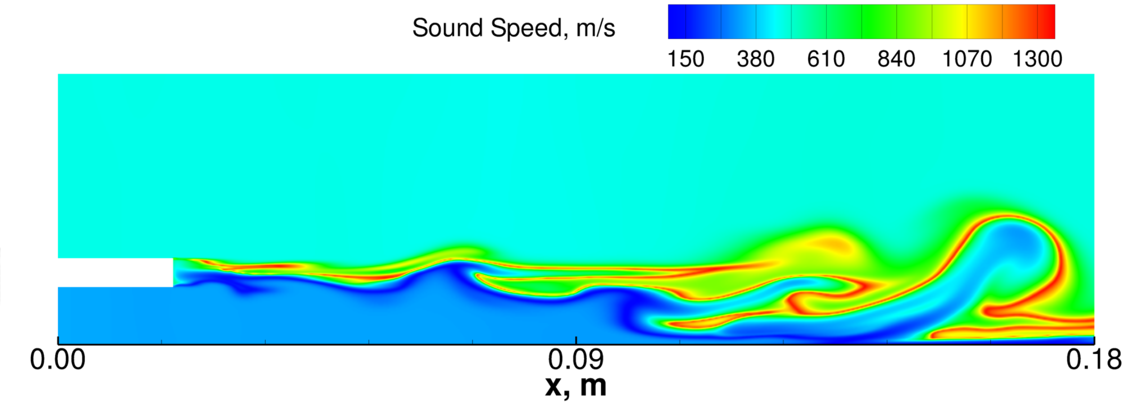

Figure 4: Sound speed for a reacting shear layer computed with the Peng Robinson equation of state.

be the compressibility of species i, then for Dalton's law the partial pressure of a gas is,

$$p_i V = n_i R T Z_i(p_i, T) \tag{27}$$

The total pressure is then,

$$pV = \sum_{i=1}^{N} n_i R T Z_i(p_i, T) \tag{28}$$

For the mixture,

$$pV = nRTZ \tag{29}$$

$$Z = \frac{pV}{nRT} \tag{30}$$

Using the definition of pressure in equation 30,

$$Z = \frac{\sum_{i=1}^{N} n_i R T Z_i(p_i, T)}{nRT} = \sum_{i=1}^{N} X_i Z_i(p_i, T) \tag{31}$$

Where X_i is the mole fraction, $\frac{n_i}{n}$. Thus the mixture compressibility is the mole weighted average of the individual compressibilities. The individual compressibilities are evaluated at the mixture temperature and the partial pressure of individual species. Amagat's law of partial volumes states that,

$$V = \sum_{i=1}^{N} V_i \tag{32}$$

where V_i is the partial volume of species i in the mixture. Using a similar procedure the partial volume of each species is,

$$pV_i = n_i R T Z_i(p, T) \tag{33}$$

For the mixture this results in,

$$Z = \frac{p \sum_{i=1}^{N} n_i R T Z_i(p, T)}{nRT} = \sum_{i=1}^{N} X_i Z_i(p, T) \tag{34}$$

The key difference with Amagat's Law is that the compressibility of each species is a function of the mixture pressure, not the partial pressure of the individual species. To illustrate this difference, the mixture compressibility is calculated using the traditional Peng Robinson equation of state, and the Peng Robinson equation of state using Dalton and Amagat's laws. A mixture of 60% CH_4 and 40% O_2 by mass at a temperature of 273 K is used. The results are shown in Figure 5. It is clear that except at very low pressures the ideal gas equation of state yields incorrect values. The traditional Peng Robinson model and the Amagat's model provide very close agreement at all points. Dalton's mixing rule provides reasonable agreement below 20 MPa but diverges significantly as the pressure is increased further. At the highest pressure, the percent error between Amagat's law and Peng Robinson is 0.18%. The percent error for Dalton's law and the ideal gas equation of state is 23.81% and 42.0% respectively. This example shows that Amagat's mixing rule should be used for non-ideal gases and provides reasonable agreement with the traditional Peng Robinson model.

Theoretically Dalton's law corresponds to the case where the compressibility of each component of the mixture assumes that only that component is present in the computation of the compressibility. Amagat's law on the other hand assumes that the influence of two unlike molecules is the same as the influence of two like molecules, this too is an approximation of the real behavior. In the case of a true real gas mixture the influence between two unlike molecules does not have to be the same as the influence of two like molecules [**?**]. In practice this unlike interaction can be introduced with an interaction index in equation 2, however data for these interaction indices is limited.

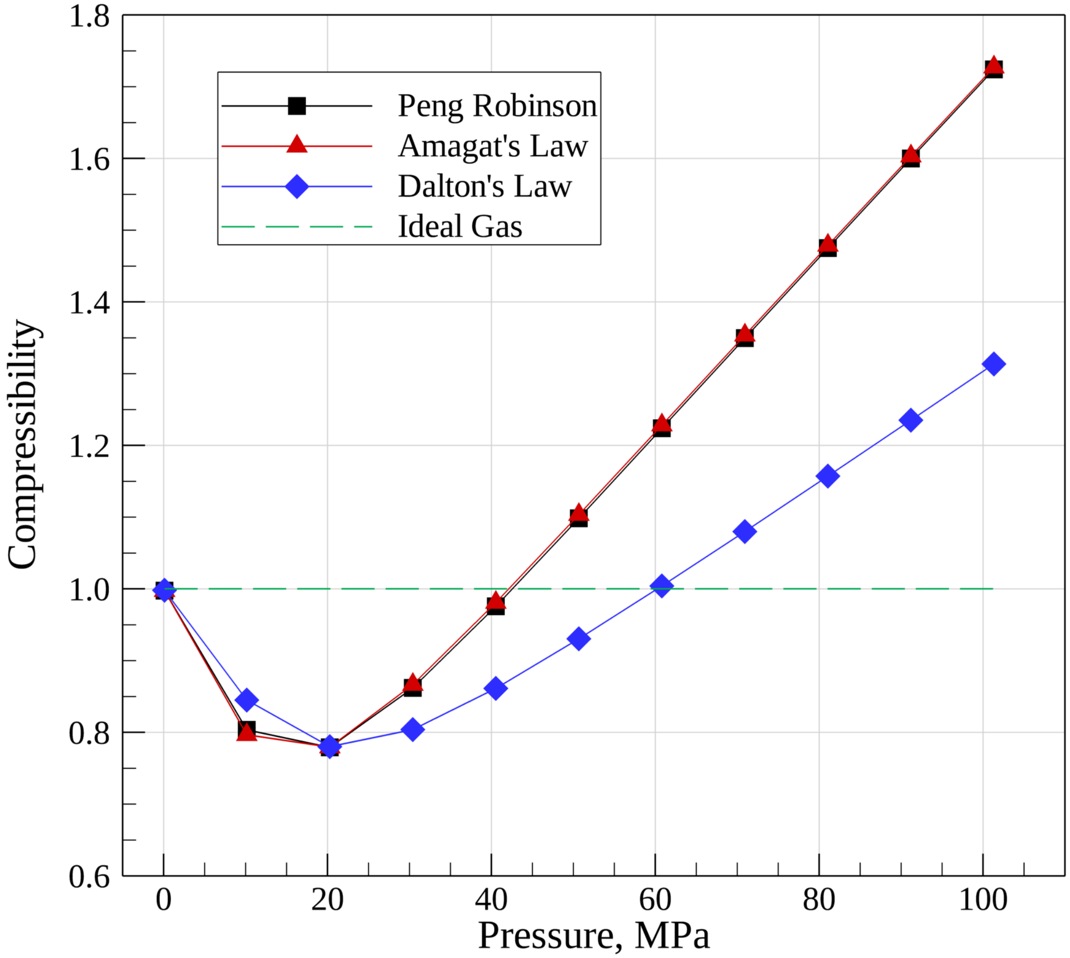

Figure 5: Mixture compressibility for a mixture of 60% CH_4 and 40% O_2 by mass at a temperature of 273 K. The mixture compressibility is computed using the traditional Peng Robinson equation of state, Dalton's law of partial pressures, Amagat's law of partial volumes and the ideal gas equation of state.

AMAGAT'S MIXING RULE

This section develops a mixing rule based on Amagat's Law using the Peng Robinson equation of state for individual species. The previous section already showed that the mixture averaged compressibility is a mole fraction weighted average of the individual species compressibilities. This means that the density is,

$$\rho = \frac{p}{RT}\left(\sum_{i=1}^{N}\frac{Y_i Z_i}{W_i}\right)^{-1} \tag{35}$$

Departure functions are computed using the same equations described for Peng Robinson but are evaluated on a per species basis since each species has a unique compressibility. The specific heat, enthalpy, and Gibbs energy of a mixture are then,

$$c_p = \sum_{i=1}^{N}\left(c_{p,i}^{\mathrm{dep}} + c_{p,i}^{\mathrm{ig}}\right) \tag{36}$$

$$h = \sum_{i=1}^{N}\left(h_i^{\mathrm{dep}} + h_i^{\mathrm{ig}}\right) \tag{37}$$

$$g = \sum_{i=1}^{N}\left(g_i^{\mathrm{dep}} + g_i^{\mathrm{ig}}\right) \tag{38}$$

The advantage of this formulation is the ability to treat the phases of a single species as separate species each with their own compressibility (density).

IDEAL GAS SPECIES

In the Amagat's model each species has its own compressibility, therefore it is possible to treat a species as an ideal gas by setting the compressibility equal to unity. The main motivation for this work is the simulation of injectors. In this case the majority of the flowfield will behave as an ideal gas once combustion has taken place. Figure 6 shows a mixture of $C_{12}H_{26}$ and H_2O at 1 MPa. The mass fraction of water is varied from 20% to 0% at two temperatures, 450 K, and 600 K. This simulates the effect of water arising from combustion when fuel is still present. The density is computed in two ways. First the $C_{12}H_{26}$ and the H_2O are treated as real gases and mixed using Amagat's law. Second, the $C_{12}H_{26}$ is used a real gas and the H_2O is treated as an ideal gas ($Z = 1$). At 450 K the difference in the density computation is noticeable, even for small amounts of water; for 5% water the density is 37% less. At 600 K the difference is less noticeable, just 11% less. This makes sense because as the temperature increases, the compressibility of water approaches unity. At 450 K it is just 0.0653 while at 600 K it is 0.738. The main motivation for this approach is to alleviate the difficulty that arises when small amount of water are added to relatively cold reactants and force the mixture to become subcritical.

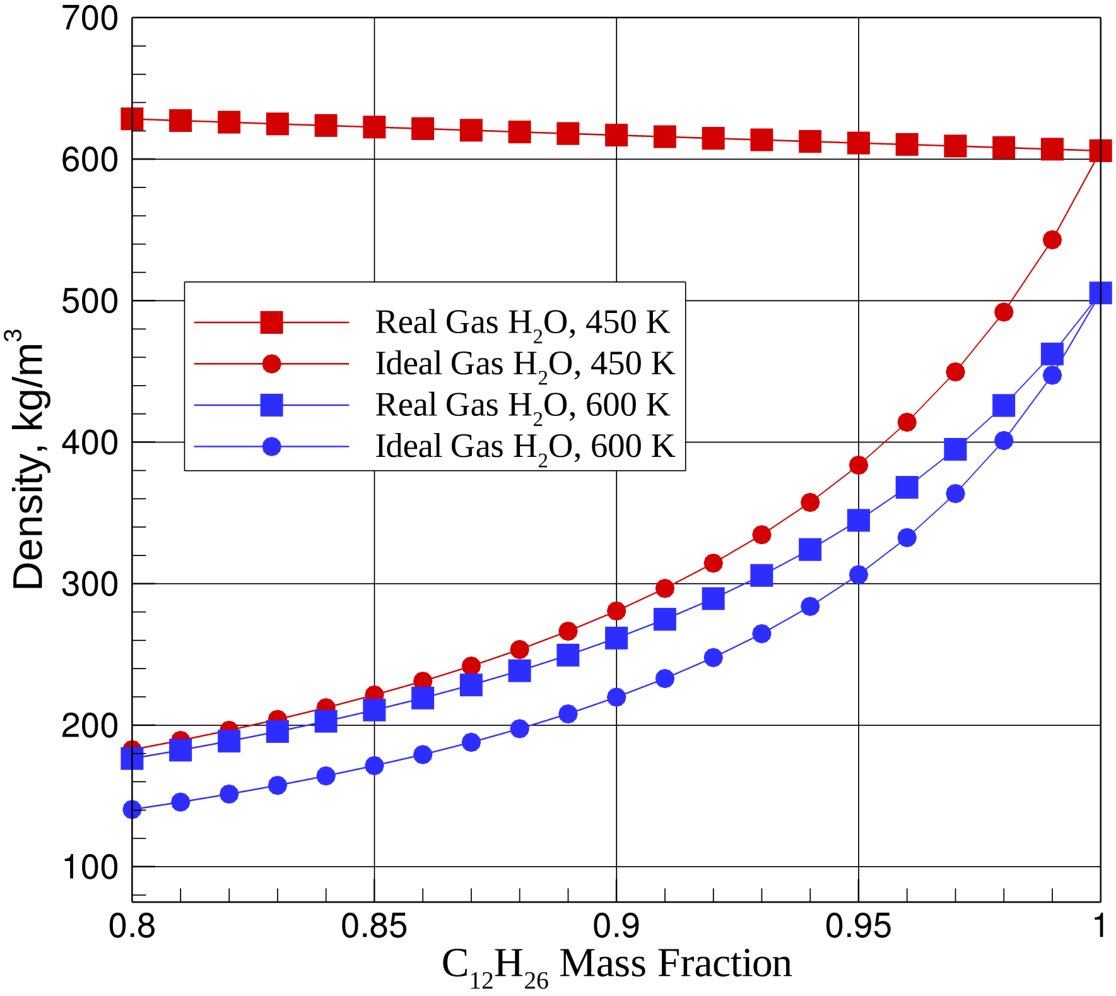

Figure 6: Density of a mixture of $C_{12}H_{26}$ and H_2O at 1 MPa. The mass fraction of water is varied from 20% to 0% at two temperatures, 450 K, and 600 K. H_2O is treated as a real gas and as an ideal gas in the two computations.

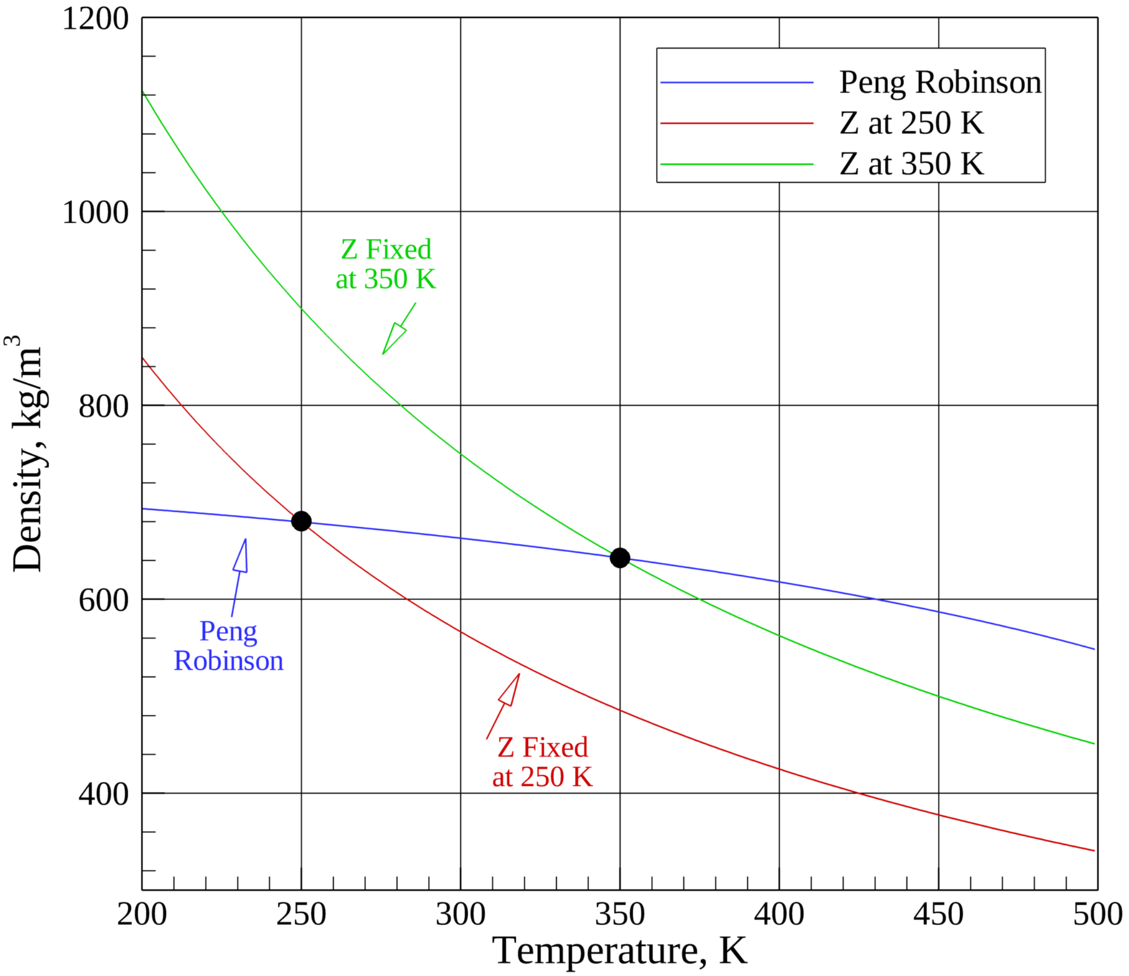

Figure 7: Density of $C_{12}H_{26}$ at 10 MPa. The density is computed using the Peng Robinson equation of state and using the ideal gas equation of state with fixed compressibility, the compressibility is computed at 250 K and 350 K.

CONSTANT COMPRESSIBILITY

An alternate approach is to apply a constant compressibility. For a uniform pressure and temperature flow this would result in the correct velocity at the inlet when was the mass flow is specified. The applicability of this is less effective as the temperature and pressure vary. Figure 7 illustrates this by showing the density of $C_{12}H_{26}$ at 10 MPa. The density is computed using the Peng Robinson equation of state and using the ideal gas equation of state with a fixed compressibility. The fixed compressibility is defined using the real gas density at two different temperatures, 250 K and 350 K. It is clear that away from the point where the compressibility was defined the difference is large. This is because the shape of the density curve for a real gas and an ideal gas is different. The inclusion of a compressibility simply shifts the ideal curve up or down, it does not alter the shape. This method should only be applied for flows that are approximately isothermal, or where the species is consumed quickly. A potential application of this is an injector where the fuel is quickly consumed before rapid temperature changes take place.

LIQUID SPECIES AND PHASE CHANGE

One of the initial motivations for the Amagat's mixing rule based version of Peng Robinson was to allow for the treatment of the liquid and vapor states as separate species. By choosing the compressibility based on the minimum value the liquid density can be preserved for a longer duration. Figure 2 showed the roots of the Peng Robinson equation of state. The compressibility is typically taken to be the maximum root. For the case shown the transition away from liquid behavior to gaseous behavior would occur at around 310 K. If the minimum root is used instead the liquid behavior wouldnt occur until close to 600 K. The benefit of this approach is that one maintains more stable properties as the propellant is heated in the initial phases of combustion. The sharp jump between the liquid and gas states is avoided. To preserve the physical state of the system the liquid can then be converted into a gas over a finite rate of time. The gaseous species can then be modeled either with a real or ideal equation of state based on the previous discussion. The simplest way to transition the species is through an Arrhenius form analogous with combustion. The production of the vapor can be written as,

$$\dot{\omega}_v = \rho k Y_\ell \exp\left(-\frac{T}{T_a}\right) \tag{39}$$

where k is a proportional constant, T_a is an activation temperature and Y_ℓ is the mass fraction of the liquid. For a single species that is divided into a vapor (Y_v) and liquid (Y_ℓ) state the system of equations in the absence of convection and diffusion is,

$$\frac{\partial \rho Y_v}{\partial t} = \dot{\omega}_v \tag{40}$$

$$Y_\ell = 1 - Y_v \tag{41}$$

An approximate solution to this system of equations for a fixed density is,

$$\rho Y_v(t) \approx \rho\left[1 - \exp\left(-k e^{-T/T_a} t\right)\right] \tag{42}$$

This equation as the correct steady state behavior,

$$\lim_{t\to\infty} \rho Y_v(t) = \rho \tag{43}$$

The actual solution will be a deviation from this since the density is a function of the composition and temperature, but this provides an initial starting point to estimate the parameters k and Ta. Figure 8 shows the solution plotted for several values of k and T_a at a fixed temperature of 450 K. As expected the solution is relatively insensitive to T_a and very sensitive to k. Larger values of k result in faster transitions between the two states.

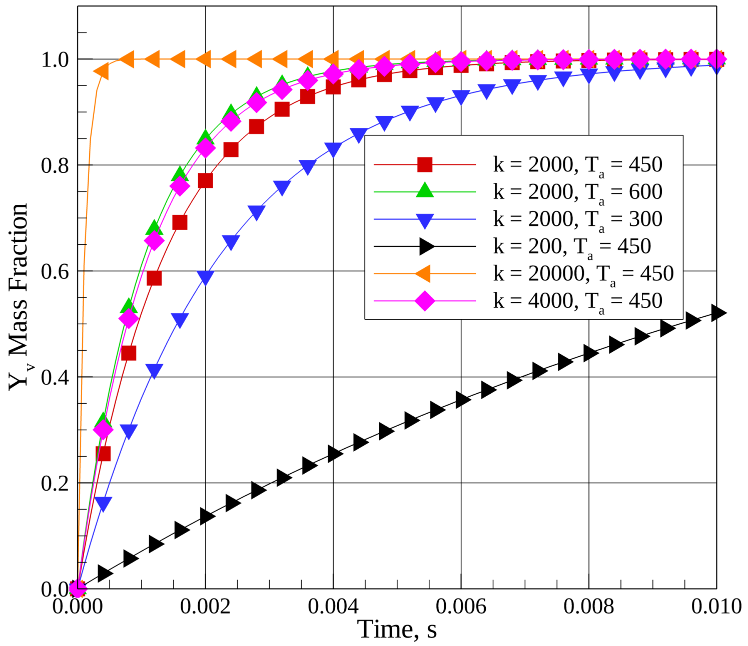

Figure 8: Solutions to equation 42 for various values of k and T_a. The solution is sensitive to k and insensitive to T_a.

DEMONSTRATION CASES

SINGLE SPECIES WITH HEAT ADDITION

To evaluate the constant compressibility model a constant area duct is used, $C_{12}H_{26}$ is injected into the duct at 250 K at a mass flow rate of $350\,\mathrm{kg/s \cdot m}$. The temperature in the duct rises as the flow moves down stream due to a volumetric heat source. The compressibility at the inlet conditions is 1.86. In practice using this compressibility will not give the correct density because other flowfield aspects, like the pressure, will change and alter the density. To get the exact density at the inlet with a fixed compressibility an iterative process is needed. In this case a compressibility of 3.1 will match the real gas density at the inlet. Figure9 shows the heat addition profile along with profiles of the density, sound speed, and velocity. The heat addition is the same for each simulation. Four curves are plotted which show the results for an ideal gas equation of state, fixed compressibility of 1.86, fixed compressibility of 3.1, and the Peng Robinson solution. When the compressibility of 3.1 is used the initial density and velocity match the real gas solution. Once the heat addition is activated at 0.02 m, the profiles diverge significantly, in the ideal gas simulations the density decreases rapidly compared to the real gas simulation. It is also clear that all of the ideal gas based simulations provide an incorrect sound speed predictions at low temperatures. This will affect instability and wave speed propagation times. In a simulation where burning is taking place, it is expected that the $C_{12}H_{26}$ would be rapidly consumed as the temperature is increased so there is still potential applicability of this method so long as the error in the mid-temperature region is acceptable. It is clear that a careful study must be done to obtain the compressibility that will yield the desired velocity since that is the main motivation for this model.

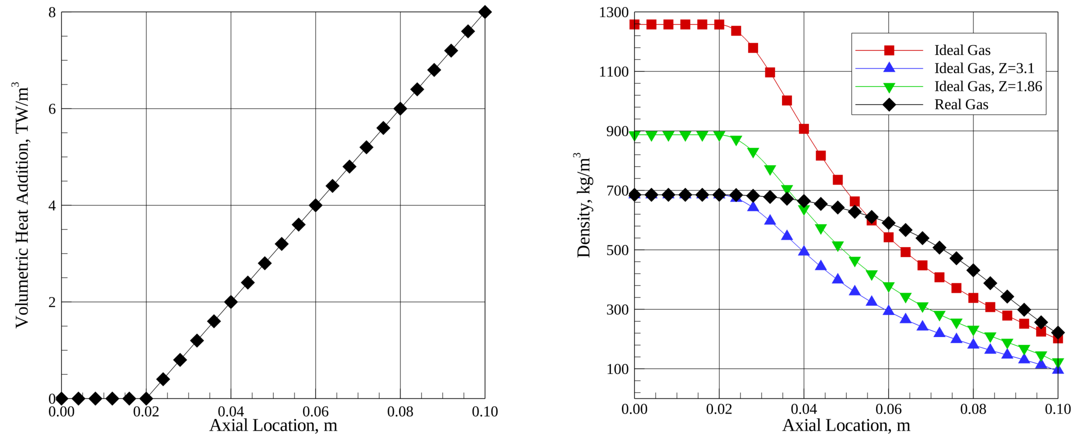

(a) Volumetric Heat Addition.

(b) Density.

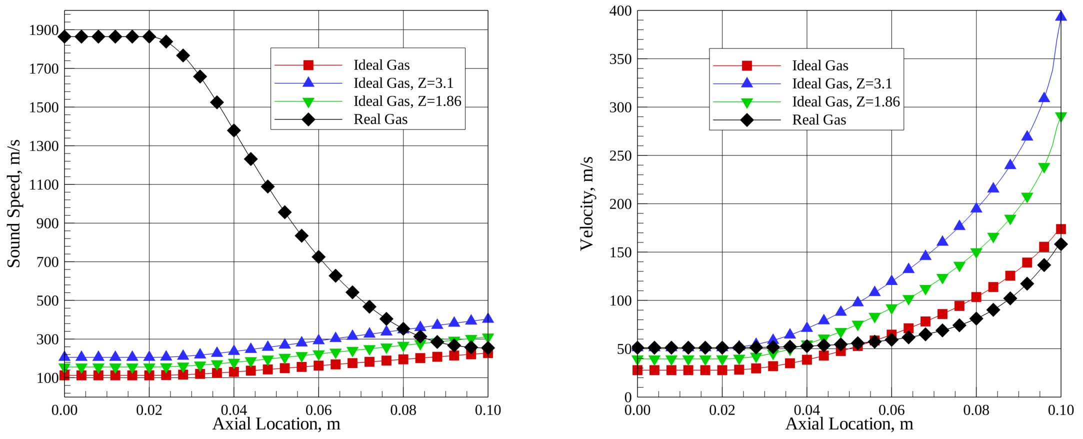

(c) Sound Speed.

(d) Velocity.

Figure 9: A constant area simulation of $C_{12}H_{26}$ with heat addition is used to evaluate the constant compressibility simplification.

MIXTURE WITH HEAT ADDITION

The same setup can also be used for a uniform mixture. For this test 40% $C_{12}H_{26}$, 40% O_2, 10% H_2O and 10% CO_2 by mass are injected at 250 K at a fixed mass flow rate of 350 kg/s · m. The heat addition is identical to the profile shown in Figure 9. The results for the mixture are shown in Figure 10. For the mixture the compressibility was not tuned, instead four different equations of state were evaluated, ideal gas, Peng Robinson, and two versions of Amagat's Mixing Rule. Amagat's Law I uses the Peng Robinson equation of state for each component while Amagat's Law II uses the ideal gas equation of state for the products, (CO_2 and H_2O). For Amagat's Law II, the compressibility is unity for the ideal gas species. On the low temperature side there is a significant difference in the density, all three approximate models show deviation from the Peng Robinson equation of state. In the high temperature region all four of the equations of state converge to a similar density. This convergence is also seen in the pressure, sound speed, and velocity. Like the previous single species case the low temperature sound speed is only correctly predicted by the full Peng Robinson equation of state. This demonstration along with the previous case shows that the other simplified models

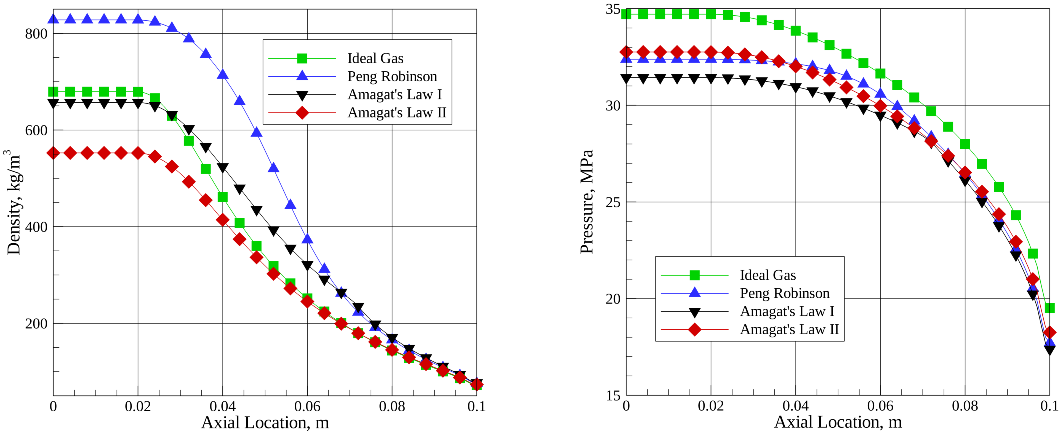

(a) Density.

(b) Pressure.

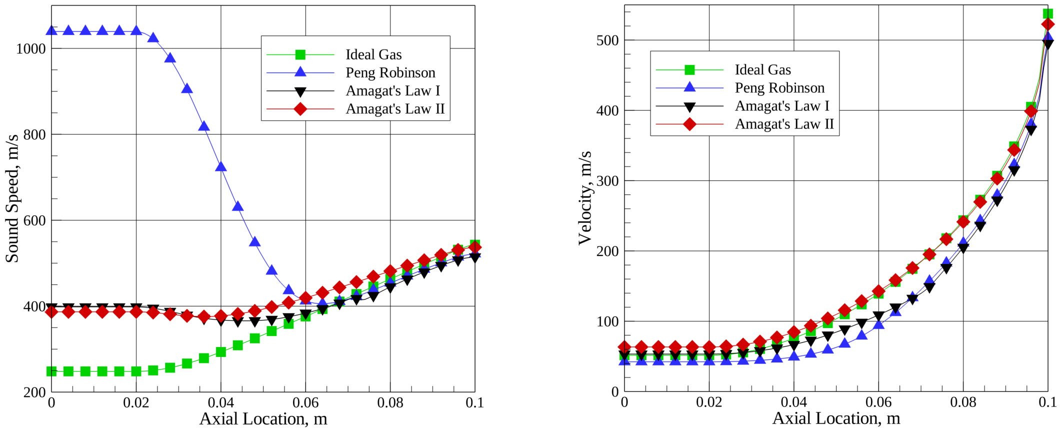

(c) Sound Speed.

(d) Velocity.

Figure 10: A constant area simulation of 40% $C_{12}H_{26}$, 40% O_2, 10% H_2O and 10% CO_2 by mass with heat addition is used to evaluate the equation of state.

can be used to match part of the Peng Robinson model, but a complete agreement is not possible.

PREMIXED COMBUSTION

To test combustion, a premixed configuration is used. A mixture of 40% $C_{12}H_{26}$ and 60% O_2 by mass is injected into a constant area duct at a mass flow rate of $5\,\mathrm{kg/s \cdot m}$ at a temperature of 610 K. The simulation is run for 0.75 s using the same four equations of state that were evaluated in the previous case. A simple two-step combustion mechanism is used for the dodecane combustion. Figure 11 shows the results of the four simulations. Excluding the ideal gas equation of state, the other three versions show very similar results. Predictions of the density are off slightly before combustion takes place but during the early stages of combustion which are taking place in the downstream region the densities are very similar between Peng Robinson and the two Amagat's based mixing rules.

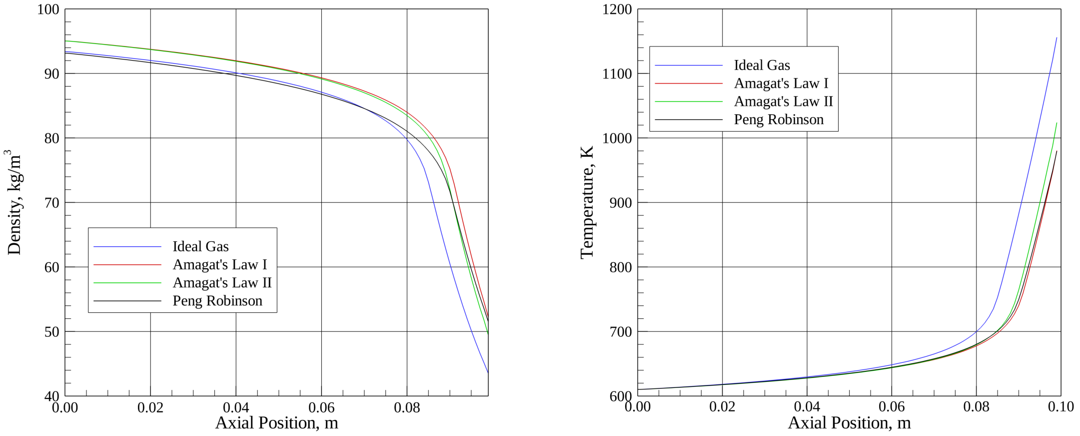

(a) Density.

(b) Temperature.

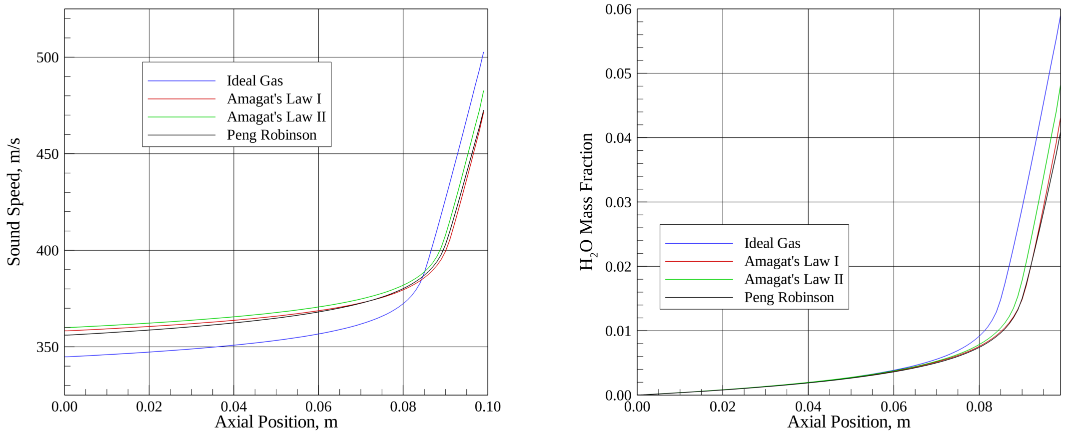

(c) Sound Speed.

(d) H_2O Mass Fraction.

Figure 11: Premixed combustion results. A mixture of 40% $C_{12}H_{26}$ and 60% O_2 by mass at 610 K is injected at a mass flow rate of $5\,\mathrm{kg/s \cdot m}$. Results are shown after 0.75 s.

NON-PREMIXED COMBUSTION

A two-dimensional shear layer representative of a $C_{12}H_{26}$ injector is used to test the Peng Robinson Amagats mixing model and the fixed compressibility model. For this simulation, a code which is second order accurate in time and space is used. The mesh contains approximately 250,000 cells and has uniform spacing. The fuel is $C_{12}H_{26}$ and is injected at 600 K with a mass flow rate of $75\,\mathrm{kg/s \cdot m}$, the oxidizer is pure O_2 and is injected at 610 K with a mass flow rate of $150\,\mathrm{kg/s \cdot m}$. The mean pressure is 3.8 MPa. For the fuel, these conditions are supercritical in pressure but subcritical in temperature. For the oxidizer, the conditions are subcritical in pressure and supercritical in temperature. A converged solution with the pure Peng Robinson model was not obtainable.

Figure 12 shows the density for the fixed compressibility over time. The density of the fuel varies as the time progresses this is unlike the real gas which uniform density throughout time. This is due to the density of the real gas being relatively insensitive to property changes at the injection conditions, unlike the ideal gas equation of state which has typical pressure and temperature dependencies.

Figure 13 shows the fuel mass fraction and temperature at two snapshots, this can be used to identify differences in how the shear layer interface behaves for the two models. One noticeable difference is that the interface between the oxidizer and fuel is very sharp for the real gas equation of state compared with the ideal gas which shows a diffuse interface. This may effect mixing. A smooth interface will result in less vorticity generation through baroclinic torque. Despite these clear differences, the temperature plot shows a qualitatively similar combustion. A thin flame is attached to the splitter plane and extends along the interface between the fuel and oxygen.

SUMMARY AND CONCLUSIONS

A number of alternate approaches to a pure cubic equation of state were presented. The motivation for these alternate formulations is the numerical difficulty introduced by the Peng Robinson equation of state for liquid rocket injector problems. The simplest model uses a fixed compressibility along with an ideal gas equation of state. This model can be used to match the incoming velocity, but in the presence of thermal gradients and pressure changes unwanted variations in the density will occur. This is due to a fundamental difference in the shape of the density curve for a real gas and an ideal gas in the non-ideal region. Two versions of an equation of state based on Amagats Law were developed. One uses the Peng Robinson equation of state for all of the components, and one uses the Peng Robinson equation of state only for selected components. The complete real gas version showed excellent agreement in terms of compressibility, but differences in sound speed and other thermodynamic properties were seen in for some mixtures. Initial testing shows that both of these models are more numerically stable than the traditional Peng Robinson model, but additional work should be done to better understand and classify the assumptions and associated error with using Amagats Law, especially for mixtures of unlike gases where the grates difference is expected to occur. The final model which allowed for the use of a change in phase between liquid and vapor states had numerically stability issues and still needs further development to increase robustness, this does appear to be a potential viable option for future computations.

In addition to physical model improvements a more robust computational framework is also needed. These simulations yield flowfields with unique and complex phenomena that have not been well characterized in terms of typical numerical schemes. Recent work by Ma et al. which looked at numerical schemes for real gases should be further developed in conjunction with the current work with the ultimate goal being a more robust numerical framework for injector modeling [**?**]. The initial work on cubic equations of state was done in support of the petroleum industry, the application of these to mixtures of unlike species undergoing rapid changes in their thermochemical state due to combustion was not originally conceived. Fundamental work needs to be done to ensure that these equations are physically sound for the present application.

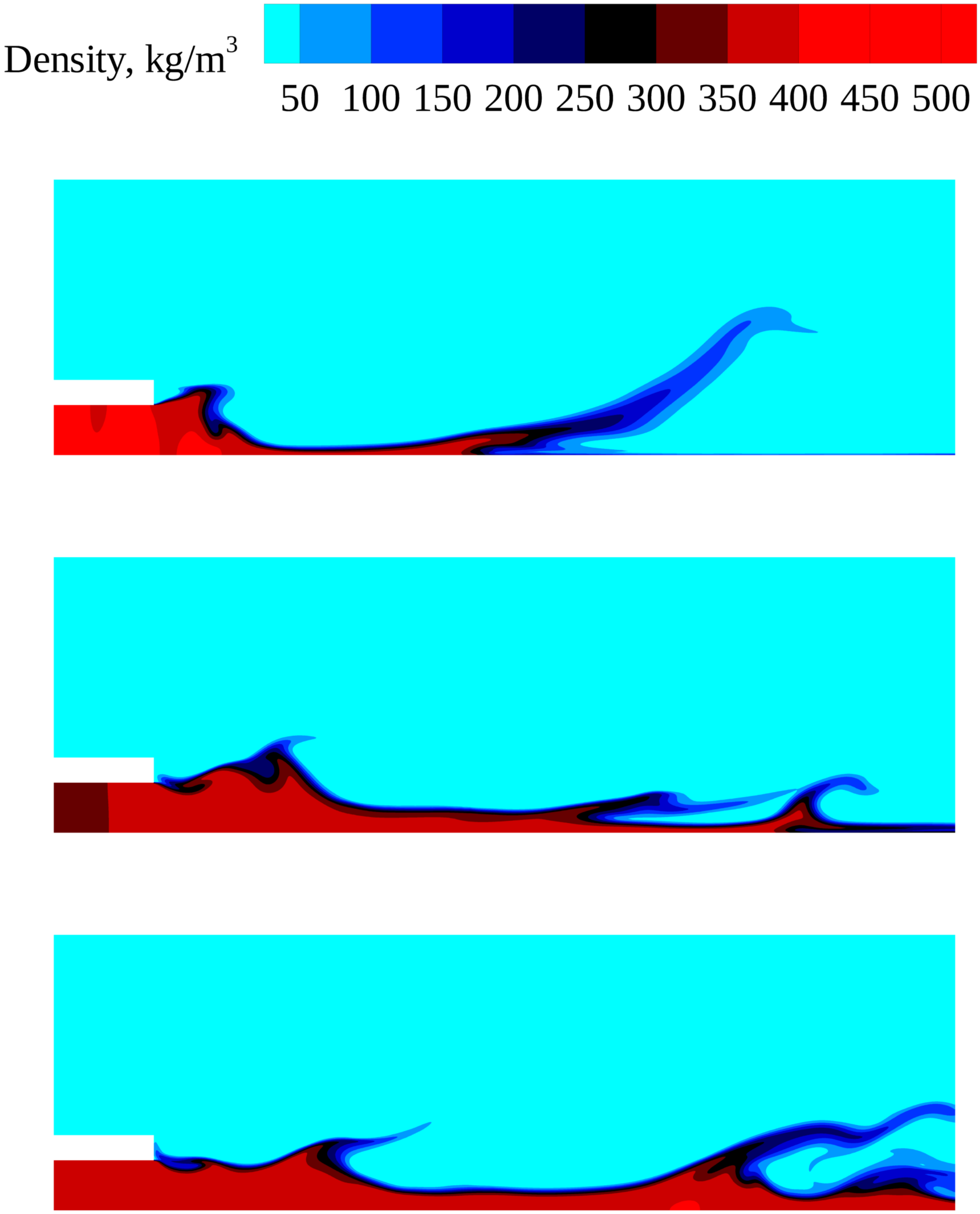

Figure 12: Density plots for the reacting shearlayer test case using the fixed compressibility model.

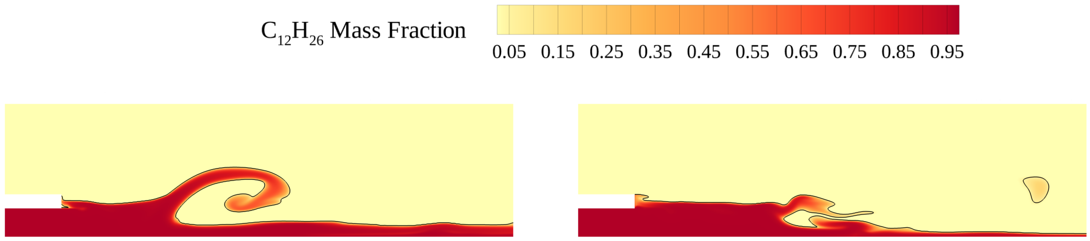

(a) $C_{12}H_{26}$ mass fraction, fixed compressibility.

(b) $C_{12}H_{26}$ mass fraction, Amagat's law.

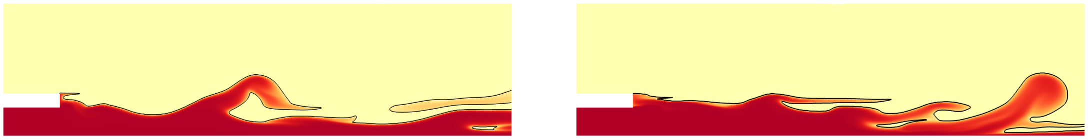

(c) $C_{12}H_{26}$ mass fraction, fixed compressibility.

(d) $C_{12}H_{26}$ mass fraction, Amagat's law.

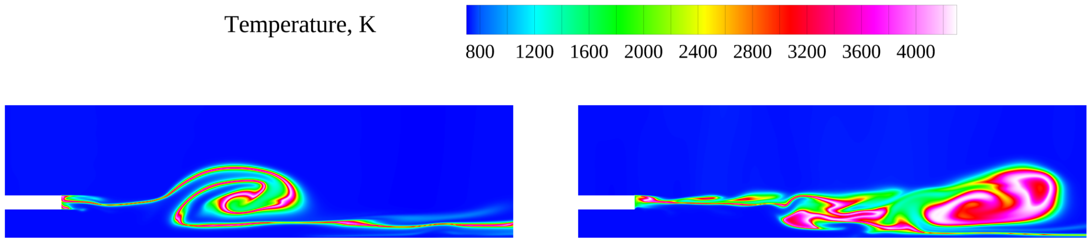

(e) Temperature, fixed compressibility.

(f) Temperature, Amagat's law.

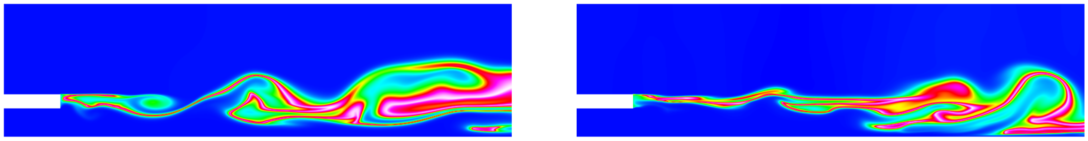

(g) Temperature, fixed compressibility.

(h) Temperature, Amagat's law.

Figure 13: $C_{12}H_{26}$ mass fraction and temperature plots for the reacting shearlayer test case.

REFERENCES

[1] M. Benedict, G. B. Webb, and L. C. Rubin, "An empirical equation for thermodynamic properties of light hydrocarbons and their mixtures ii. mixtures of methane, ethane, propane, and n-butane," *The Journal of Chemical Physics*, vol. 10, no. 12, pp. 747–758, 1942.

[2] B. Chehroudi, D. Talley, and E. Coy, "Initial growth rate and visual characteristics of a round jet into a sub- to supercritical enviroment of relevance to rocket, gas turbine, and diesel engines," in *37th AIAA Aerospace Sciences Meeting*, (Reno, NV), January 1999. AIAA Paper 1999-0206.

[3] B. Chehroudi, D. Talley, and E. Coy, "Visual characteristics and initial growth of round cryogenic jets at subcritical and supercritical pressures," *Physics of Fluids*, vol. 2, pp. 850–861, 2002.

[4] A. Roy, C. Joly, and C. Segal, "Disintegrating supercritical jets in subcritical environments," *Journal of Fluid Mechanics*, vol. 717, pp. 193–202, 2013.

[5] N. Okong'o and J. Bellan, "Direct numerical simulation of a transitional supercritical binary mixing layer: heptane and nitrogen," *Journal of Fluid Mechanics*, vol. 464, pp. 1–34, 2002.

[6] E. Masi, J. Bellan, K. Harstad, and N. Okong'o, "Multi-species turbulent mixing under supercritical-pressure conditions: modeling, direct numerical simulation and anlysis revealing species spinodal decomposition," *Journal of Fluid Mechanics*, vol. 721, pp. 578–626, 2013.

[7] J. Bellan, "Supercritical (and subcritical) fluid behavior and modeling: drops, streams, shear and mixing layers, jets and sprays," *Progress in Energy and Combustion Science*, vol. 26, pp. 329–366, 2000.

[8] J. Oefelein, "Mixing and combustion of cryogenic oxygen-hydrogen shear coaxial jet flames at supercritical pressure," *Combustion Science and Technoligy*, vol. 178, pp. 229–252, 2006.

[9] R. Dahms and J. Oefelein, "On the transition between two-phase and single-phase interface dynamics in multicomponent fluids at supercritical pressures," *Physics of Fluids*, vol. 25, pp. 1–24, 2013.

[10] D. Peng and D. Robinson, "A new two-constant equation of state," *Industrial and Engineering Chemistgry: Fundamentals*, vol. 15, pp. 59–64, 1976.

[11] B. Poling, J. Prausnitz, and J. O'Connell, *The Properties of Liquids and Gases*. New York: McGraw-Hill, fifth edition ed., 2001.

[12] B. Hoyos, "Generalized liquid volume shifts for the peng-robinson equation of state for c_1 to c_8 hydrocarbons," *Latin American Applied Research*, vol. 34, pp. 83–89, 2004.

[13] M. Harvazinski, G. Lacaze, J. Oefelein, and V. Sankaran, "Computational modeling of supercritical and transcritical flows," in *AIAA SciTech Conference*, (Dallas, TX), January 2017.

[14] K. W. Woo and S. I. Yeo, "Dalton's law vs, amagat's law for the mixture of real gases," *Center for Educational Research, Seoul National University*, pp. 127–133, 1995.

[15] P. Ma, Y. Lv, and M. Ihme, "An entropy-stable hybrid scheme for the simulation of transcritical real-fluid flows," *Journal of Computational Physics*, vol. 340, pp. 330–357, 2017.

Evaluation of Multi-Phase Equations of State for Liquid Rocket Engine Combustion Modeling

Matthew Harvazinski, Doug Talley

AFRL Rocket Lab
Edwards AFB, CA

Motivation

Enable modeling of sub-scale liquid rocket engine (LRE) injector experiments.

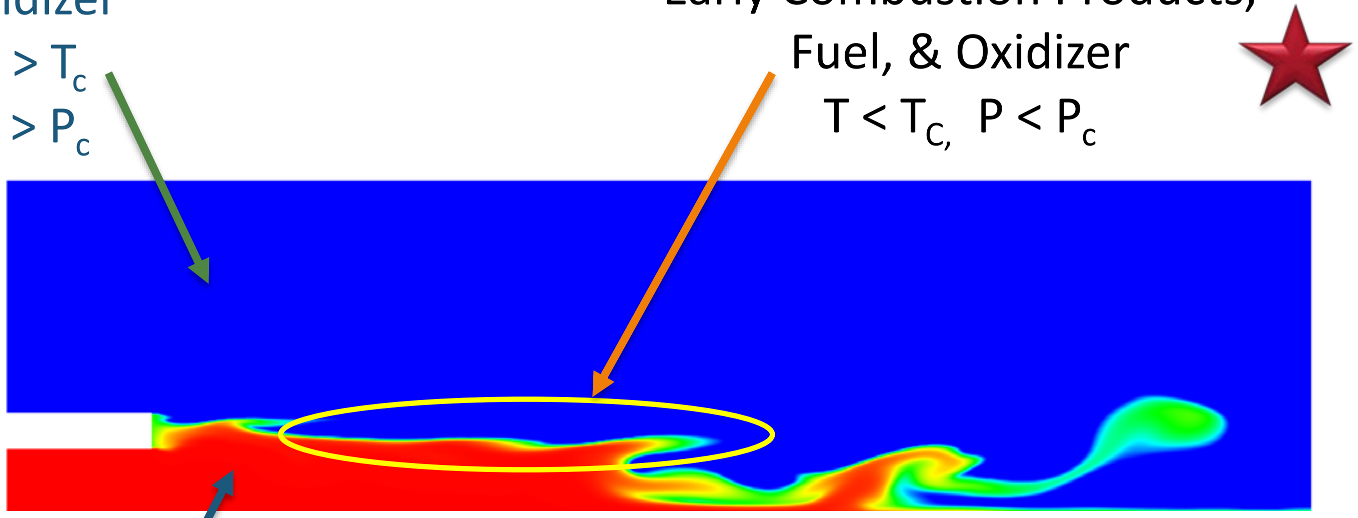

Oxidizer
$T > T_c$
$P > P_c$

Early Combustion Products,
Fuel, & Oxidizer
$T < T_{C,}\ \ P < P_c$

Complete
Combustion
Products
$T >> T_c$

Fuel
$T < T_c$
$P > P_c$

Substance	Critical Pressure P_c	Critical Temp. T_c
$C_{12}H_{26}$	1.8 MPa	658 K
O_2	5.0 MPa	155 K
H_2O	22.0 MPa	647 K

Real Gas EOS

- Peng Robinson is typically used, there are other choices
  - SRK, BWR
  - Balance between cost and accuracy
- Cubic type equations originally arose from the petroleum industry, their use in combustion modeling is questionable

Peng Robinson:

$$p = \frac{RT}{V_m - b_m} - \frac{a_m}{V_m^2 + 2b_m V_m - b_m^2}$$

a_i and b_i are functions of the critical properties (pressure and temperature) and the acentric factor for each species

Mixing Rules:

$$a_m = \sum_{j=1}^{N}\sum_{i=1}^{N} X_i X_j \sqrt{a_i a_j} k'_{ij}$$

$$b_m = \sum_{i=1}^{N} X_i b_i$$

Interaction parameter

Compressibility

- We are really after the compressibility, which is the deviation from the ideal behavior
- Solve:

$$Z^3 - (1 - B)Z^2 + (A - 2B - 3B^2)Z - (AB - B^2 - B^3) = 0$$

Mixture parameters:

$$A = a_m \frac{p}{R^2T^2}$$

$$B = b_m \frac{p}{RT}$$

$$\rho = \frac{pW}{ZRT}$$

Non-ideal correction

One compressibility per mixture.

Other Thermodynamic Properties

- Other thermodynamic properties follow from departure functions

General Form:

$$\frac{h^{\text{dep}}}{RT} = (1 - Z) + \int_V^{\infty} T \left.\frac{\partial Z}{\partial T}\right|_V \frac{dV}{V}$$

$$\frac{g^{\text{dep}}}{RT} = (1 - Z + \ln Z) + \int_V^{\infty} (1 - Z)\frac{dV}{V}$$

Peng Robinson:

$$\frac{h^{\text{dep}}}{RT} = \frac{1}{W}\left((Z - 1) + \frac{a_m - Ta'_m}{\sqrt{8}RTb_m} \ln\left\{\frac{Z/B + 1 - \sqrt{2}}{Z/B + 1 + \sqrt{2}}\right\}\right)$$

$$\frac{g^{\text{dep}}}{RT} = \frac{1}{W}\left(Z - \ln(Z - B) - 1 + \frac{a_m}{\sqrt{8}RTb_m} \ln\left\{\frac{Z/B + 1 - \sqrt{2}}{Z/B + 1 + \sqrt{2}}\right\}\right)$$

Roots to the Compressibility

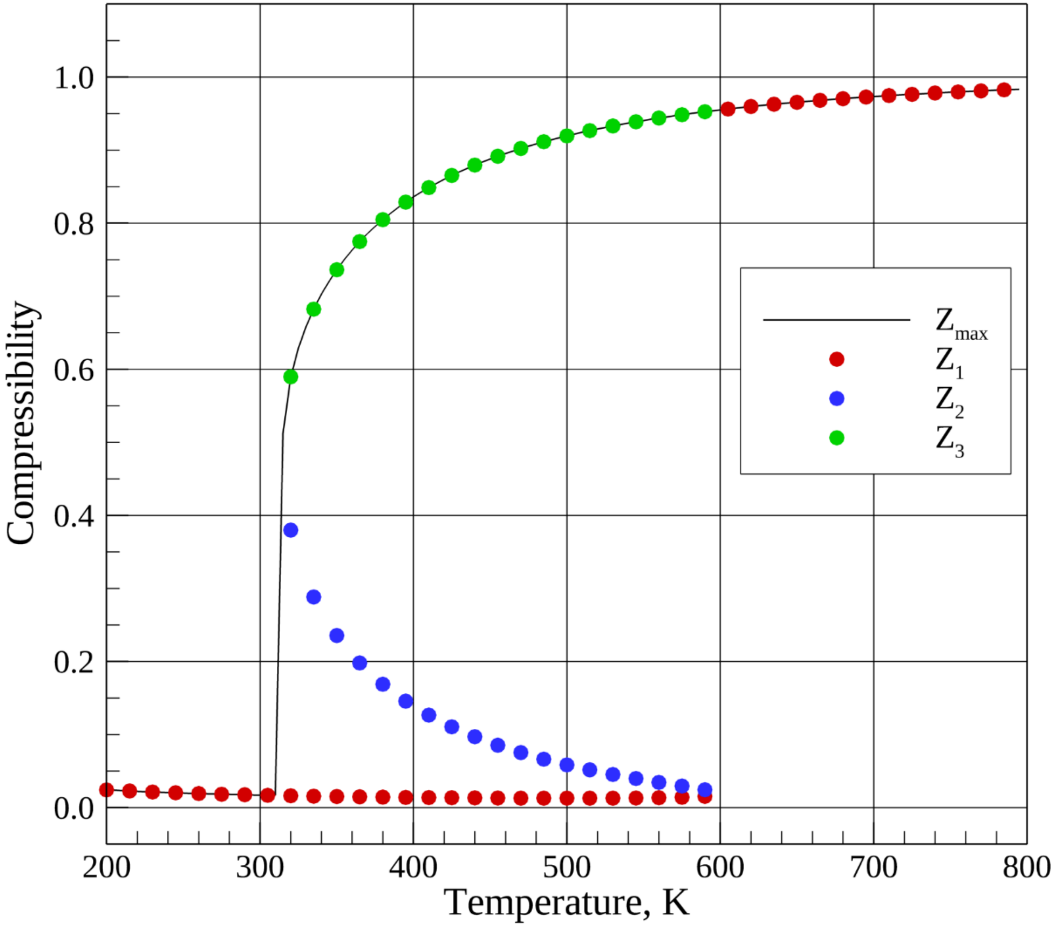

- In the multi-phase region there are three roots.
- The maximum root is used to compute the density
- The curve of the maximum root is not a smooth curve
  - Dramatic property variations
  - Numerical instability
  - No concept of quality

Challenge: sub-scale LRE

- Supercriticality is a function of pressure, temperature, and composition.
- Where the combustion products initially form, the mixture will become sub-critical and transition through the vapor dome
- The single fluid model is not valid inside the vapor dome

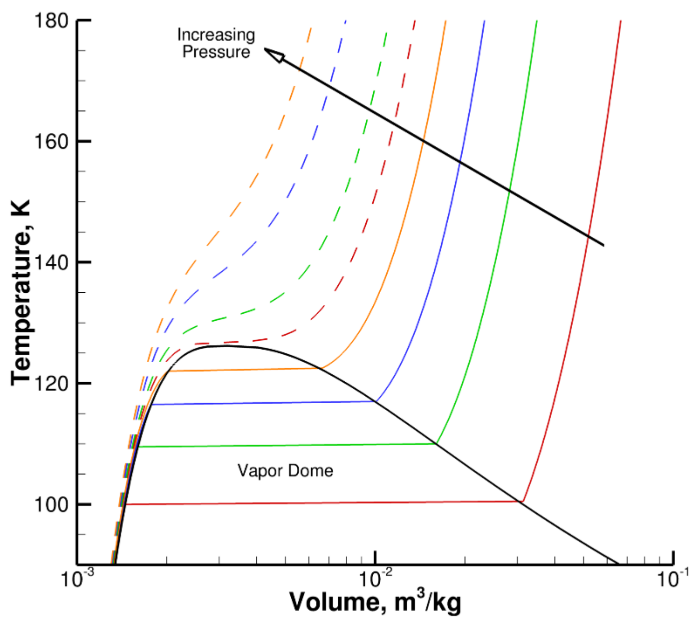

Evidence of the Dome region

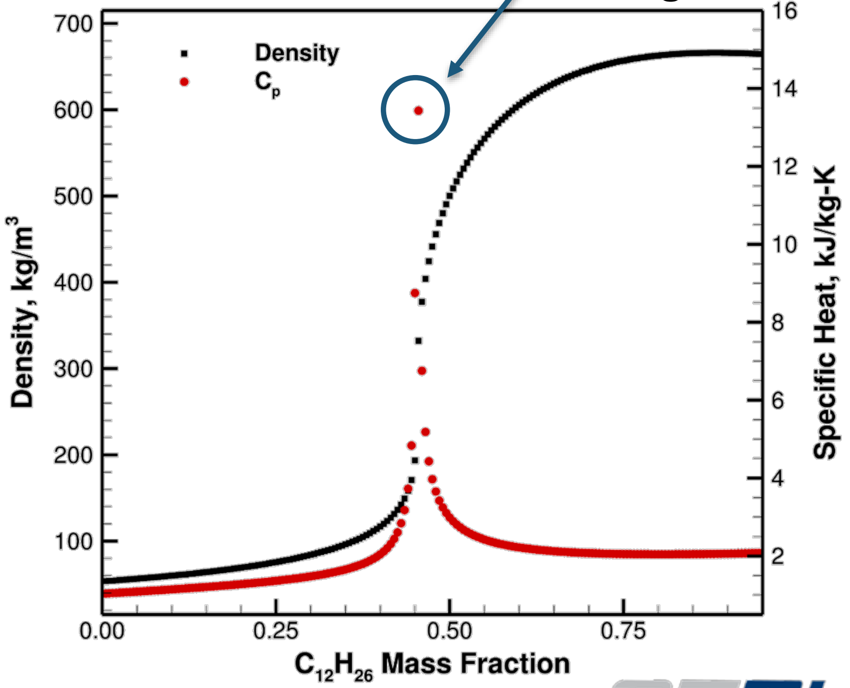

Property smoothing – tanh function

Objective – can an artificial transition through the vapor dome provide a robust model?

$$Z_s = Z_1 - \frac{Z_1 - Z_3}{2}\left[1 + \tanh G\right]$$

$$G = a_g\left\{\frac{p_{\max} Z_1 + Z_3}{1 + p_{\max}} - Z_1 + (Z_2 - Z_3)\right\}$$

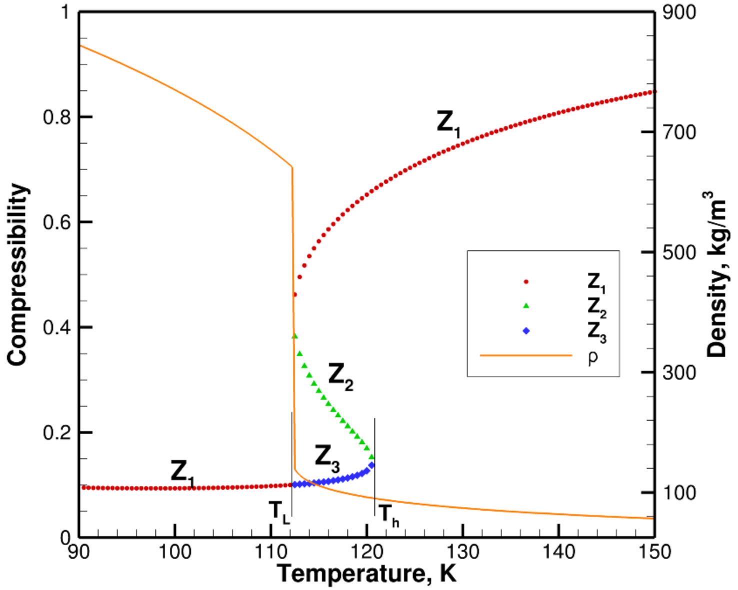

Apply this when *Z* has three real roots.

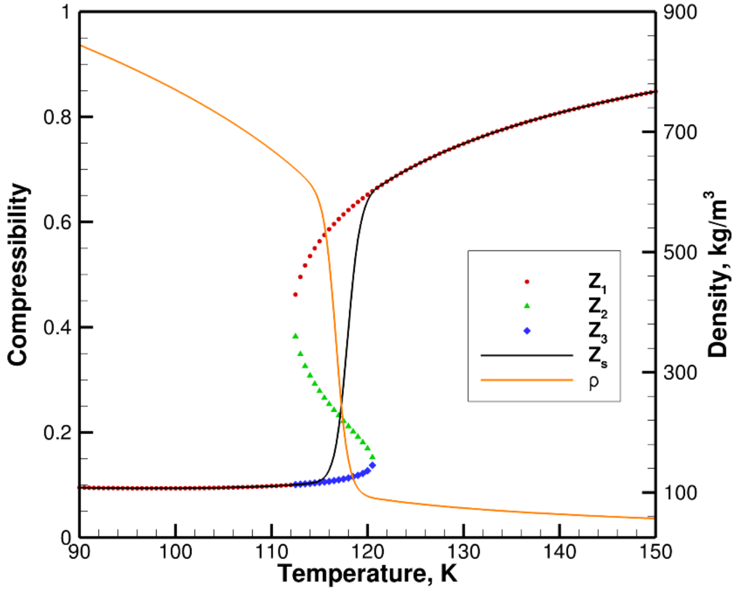

There is a unique *Z* for each *T* and *p*.

Harvazinski et al. 2017

Smoothing results for density

Pure $C_{12}H_{26}$

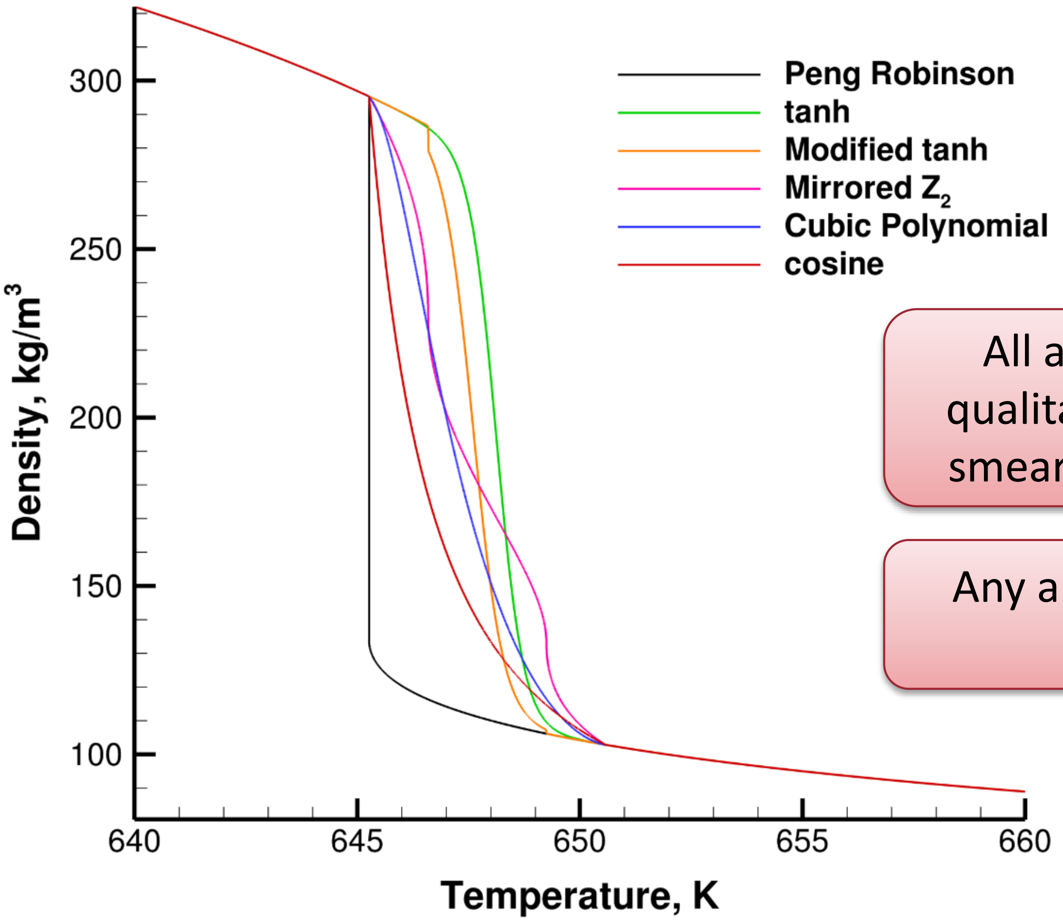

All approaches are all qualitatively similar, each smears the discontinuity.

Any approach is valid for density.

Distribution Statement A: Approved for Public Release; Distribution is Unlimited. PA Clearance Number 19064

Specific heat

Pure $C_{12}H_{26}$

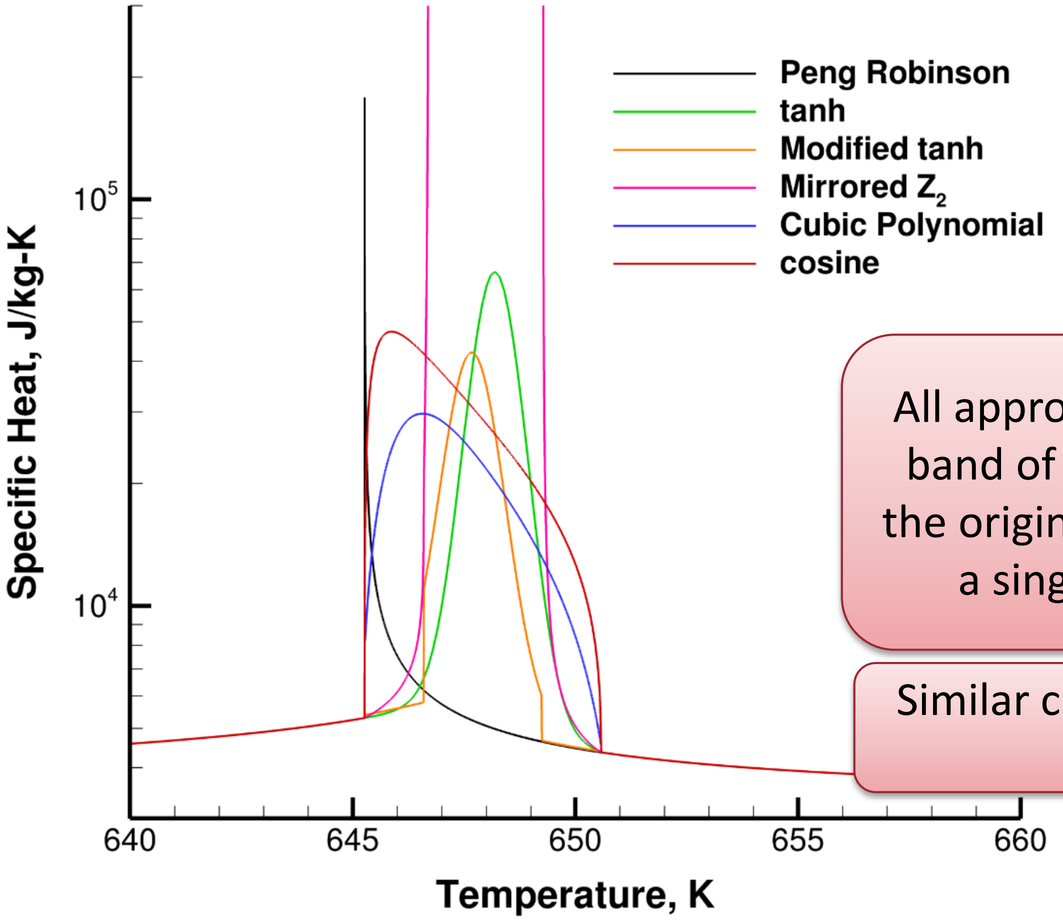

All approaches show a wide band of elevated c_p, unlike the original model which has a singular high value.

Similar challenges for sound speed.

Dalton’s and Amagat’s Law

- Dalton’s Law of partial pressures: $p = \sum_{i=1}^{N} p_i$
- Amagat’s Law of partial volumes: $V = \sum_{i=1}^{N} V_i$
- Potential alternative to the complete Peng-Robinson equation.
- If each species has it’s own Zi, how do these compare to the traditional Peng Robinson model.

Dalton’s and Amagat’s Law

- Dalton’s law is only valid for low pressures

$$Z = \frac{\sum_{i=1}^{N} n_i RT Z_i(p_i,T)}{nRT} = \sum_{i=1}^{N} X_i Z_i(p_i,T)$$

- Amagat’s law matches very well

$$Z = \frac{p\sum_{i=1}^{N} n_i RT Z_i(p,T)}{nRT} = \sum_{i=1}^{N} X_i Z_i(p,T)$$

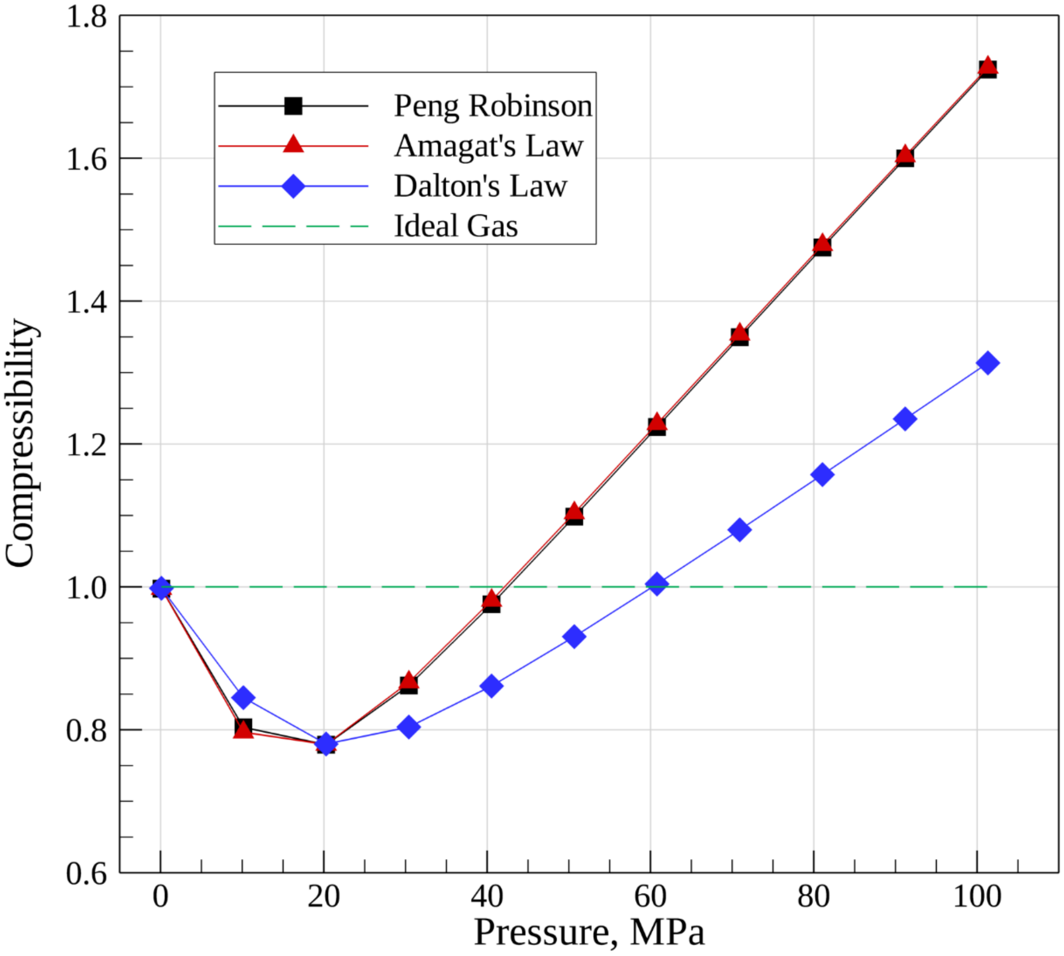

273K, 60% CH_4, 40% O_2

Amagat's Mixing Rule

- Compute a compressibility for each species
- Compute departure functions for each species
- Mixture properties are then:

$$\rho = \frac{p}{RT}\left(\sum_{i=1}^{N}\frac{Y_i Z_i}{W_i}\right)^{-1}$$

$$c_p = \sum_{i=1}^{N}\left(c_{p,i}^{\mathrm{dep}} + c_{p,i}^{\mathrm{ig}}\right)$$

$$h = \sum_{i=1}^{N}\left(h_i^{\mathrm{dep}} + h_i^{\mathrm{ig}}\right)$$

$$g = \sum_{i=1}^{N}\left(g_i^{\mathrm{dep}} + g_i^{\mathrm{ig}}\right)$$

This offers a framework to treat different species with different equations of state

Ideal Gas Species

- By setting Z_i=1, a species can be treated as an ideal gas, like water vapor in a combustion calculation

- Large deviation at lower temperatures compared to higher pressures

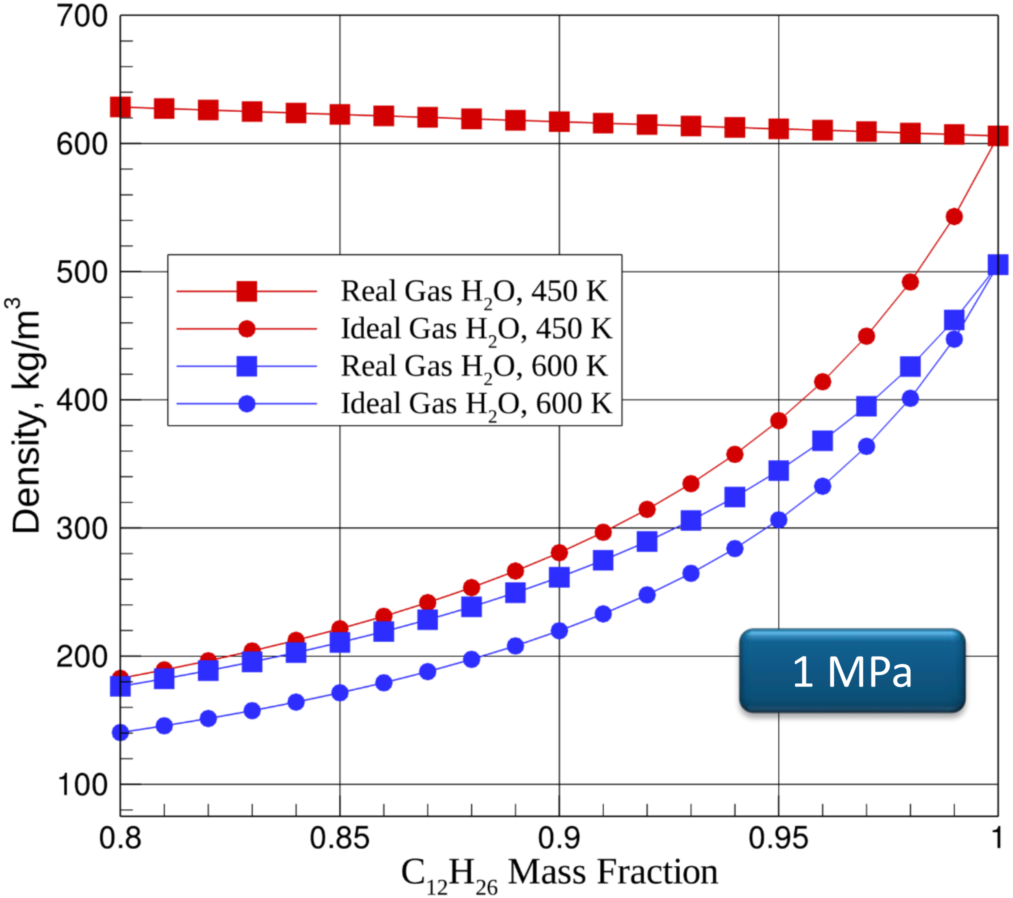

Fixed Compressibility

- Motivation: We want the correct velocity when the mass flow rate is prescribed.
- Use a scaled ideal gas equation of state
- This will not "fix" the shape of the curve

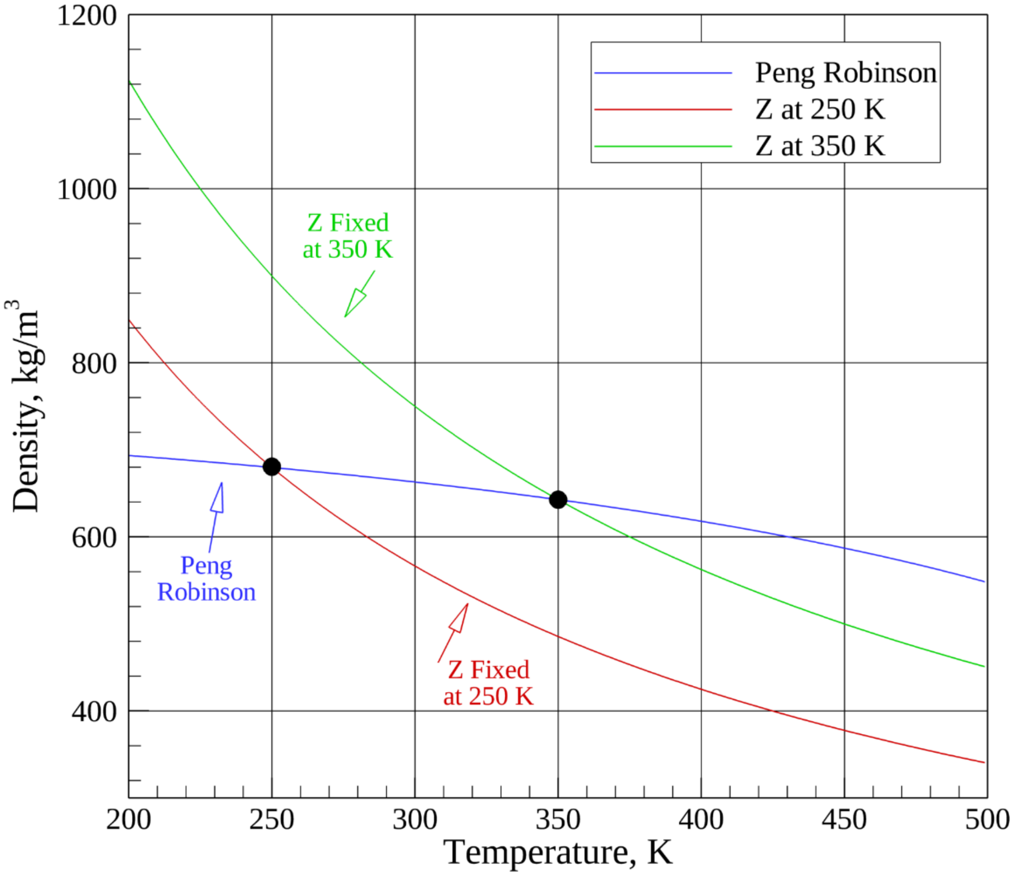

Distribution Statement A: Approved for Public Release; Distribution is Unlimited. PA Clearance Number 19064

Different Phases

- Transition from the liquid phase to the gas phase over a finite amount of time

$$\dot{\omega}_v = \rho k Y_\ell \exp\left(-\frac{T}{T_a}\right)$$

$$\rho Y_v(t) \approx \rho\left[1 - \exp\left(-k e^{-T/T_a} t\right)\right]$$

- Current formulation needs improvements for robustness

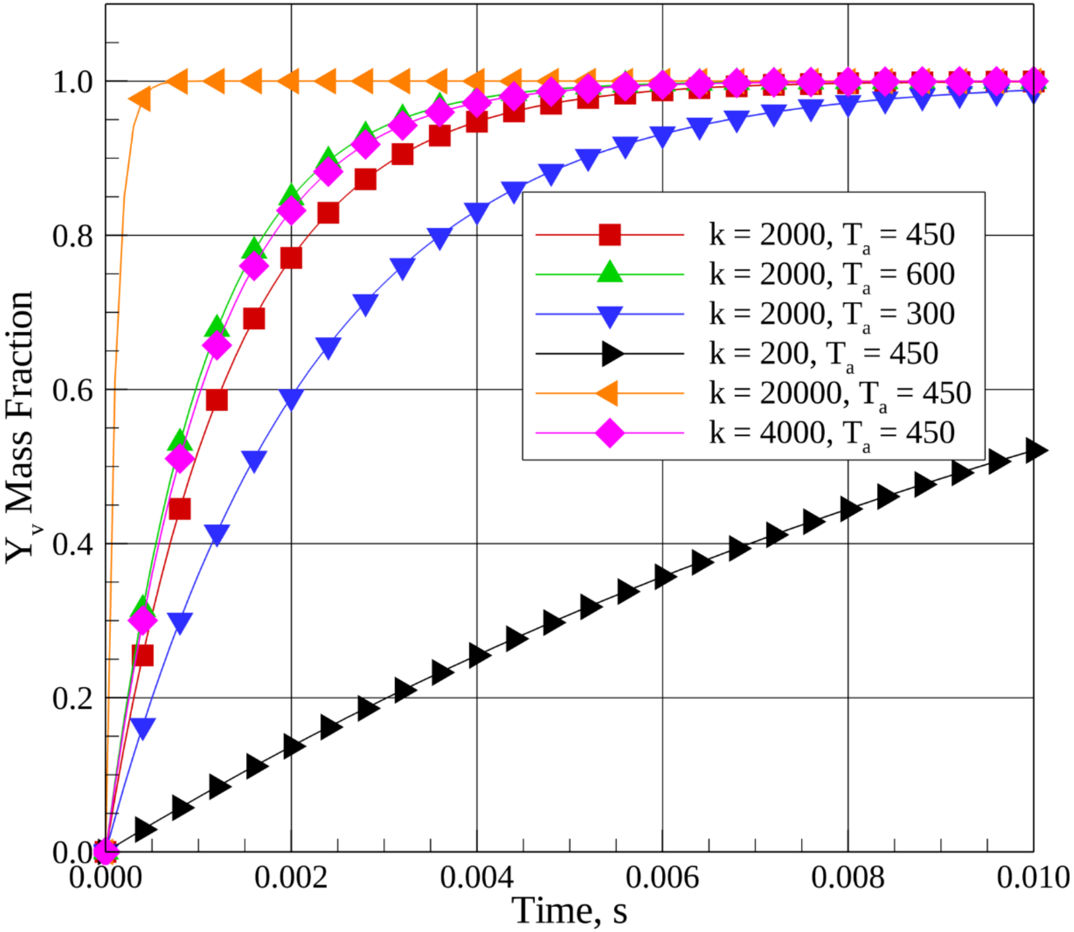

Single Species Heat Addition

- Heat addition in a uniform area duct
- Dodecane, 250 K, constant mass flow rate

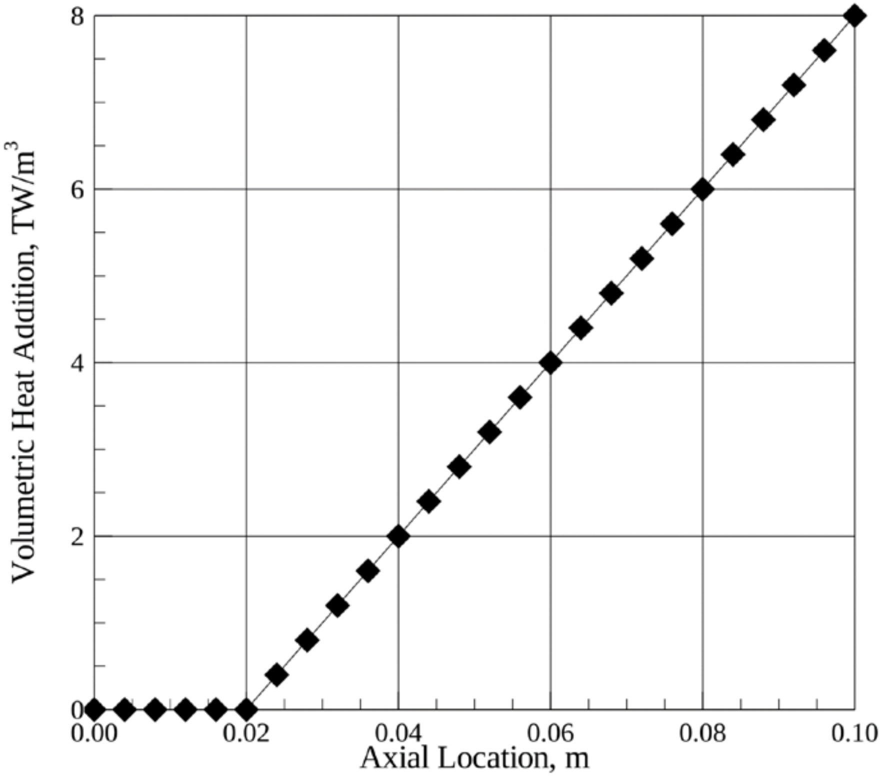

Single Species Heat Addition

- It is very difficult to “pin” the compressibility
- The computed Z is 1.86
- The actual Z which matches the density is 3.1
- Why?
  - Other flowfield (p, u) features are changing which alters the flowfield and changes the conditions
- The shape of the curve is different

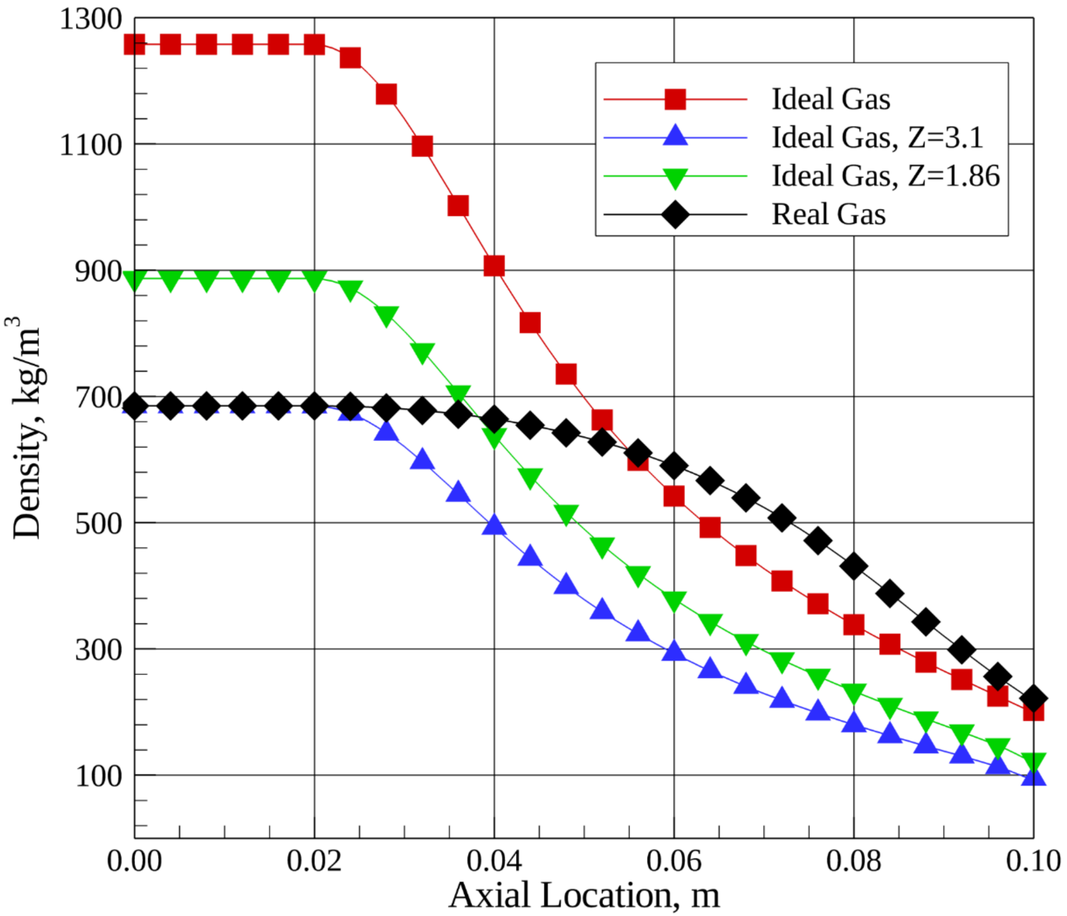

Single Species Heat Addition

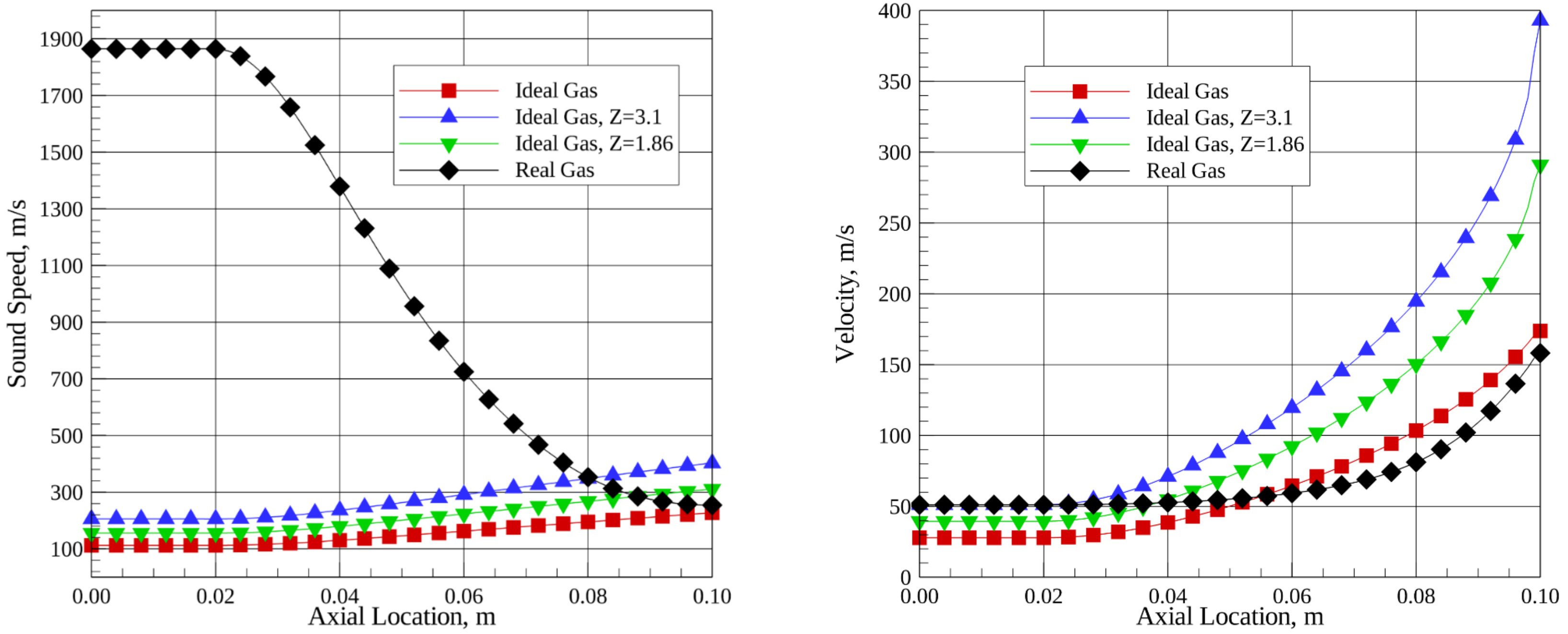

Multiple Species Heat Addition

- Heat addition in a uniform area duct
- 40% $C_{12}H_{26}$, 40% O_2, 10% H_2O, 10% CO_2, 250 K, constant mass flow rate
- Amagat's I – all components use Peng-Robinson
- Amagat's II – only $C_{12}H_{26}$ & O_2 use Peng-Robinson

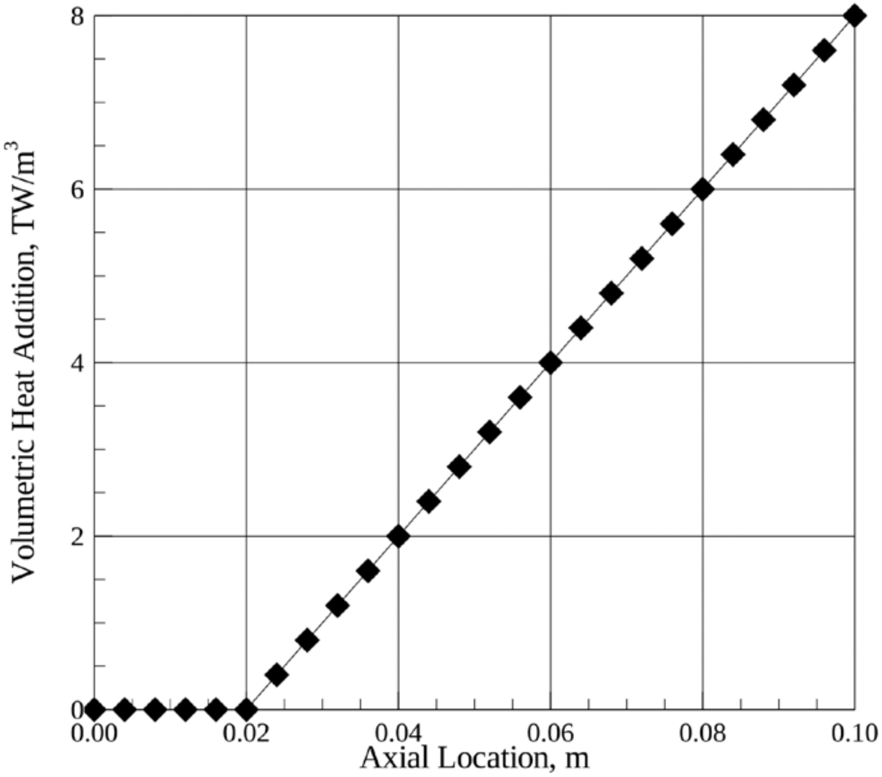

Multiple Species heat Addition

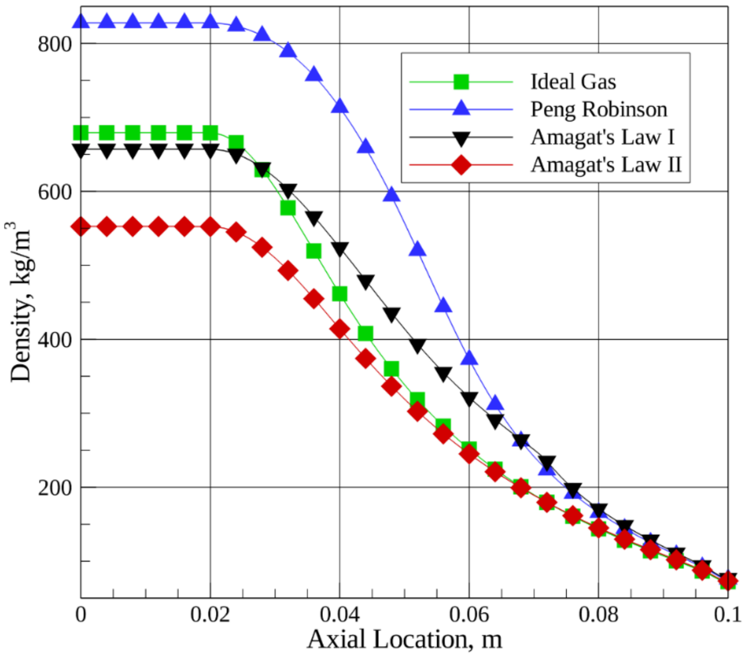

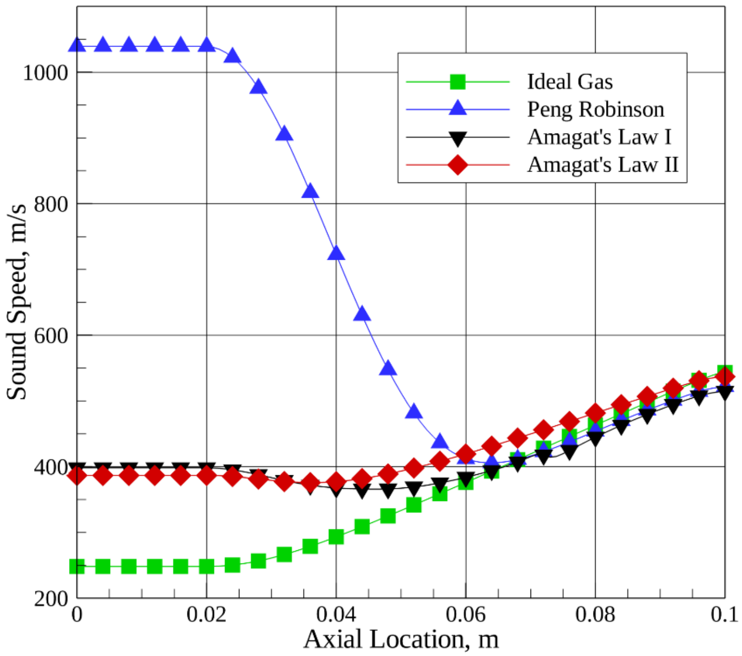

Density predictions in the high temperature region converge

Only Peng Robinson yields a “liquid like” sound speed at low temperatures

Multiple Species heat Addition

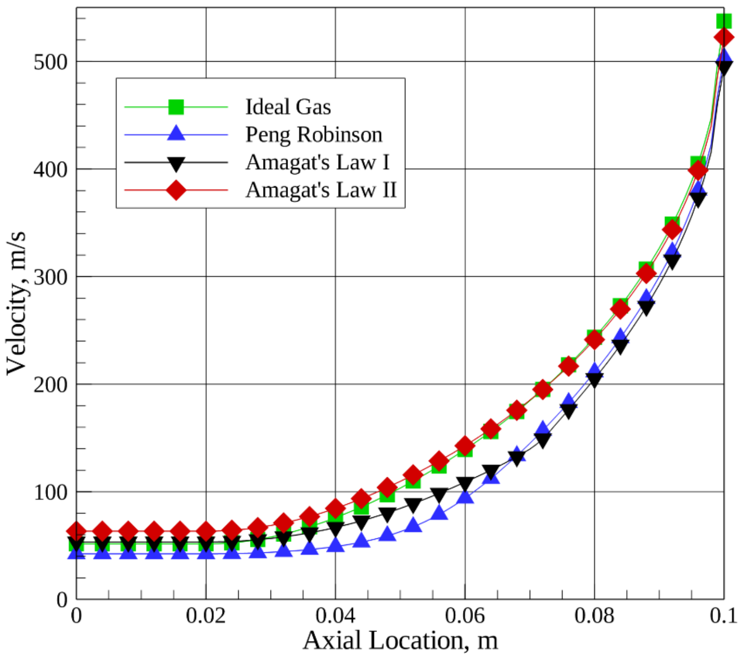

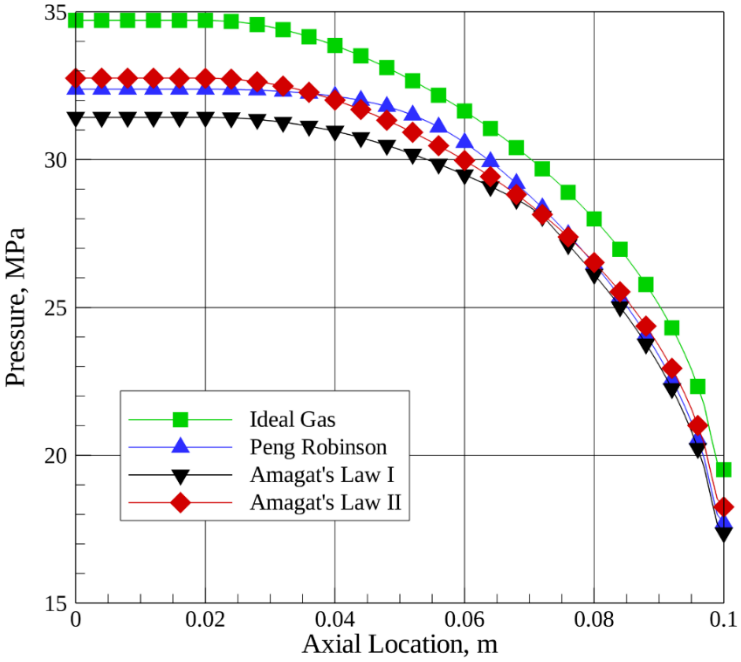

Velocity predictions are reasonable

Premixed Combustion

- Setup:
  - 5 kg/s
  - 610 K
  - 40% $C_{12}H_{26}$, 60% O_2
- The simulation is run for 0.75 s to capture the early stages of combustion

Premixed Combustion

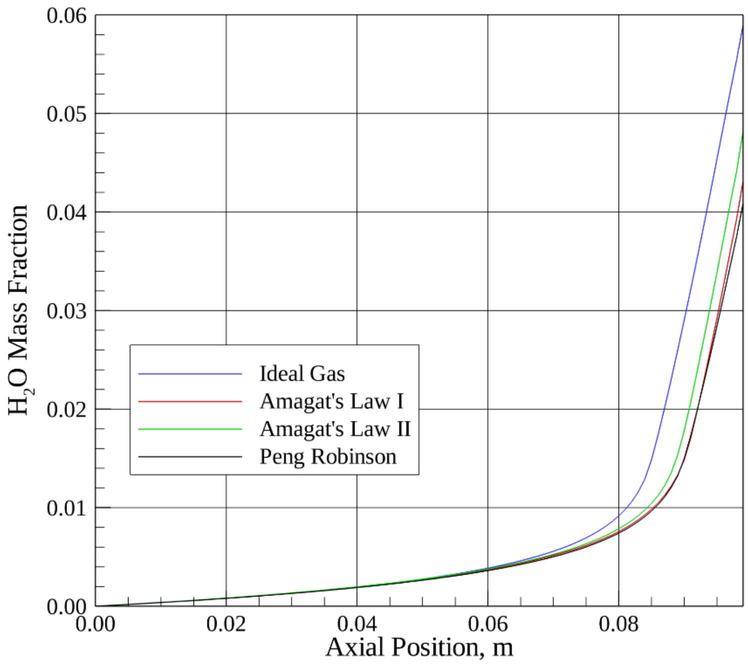

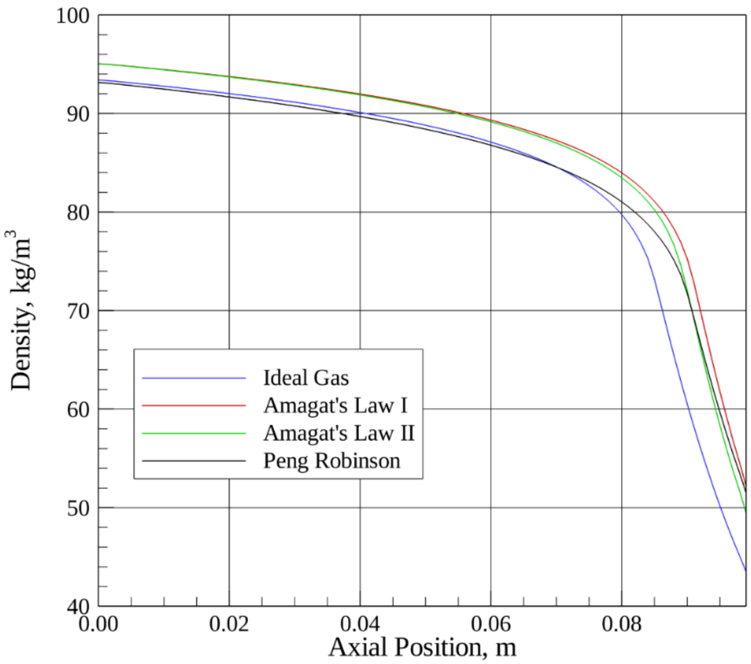

Reasonable agreement for Amagat’s Law and Peng Robinson in terms of H_2O production

Premixed Combustion

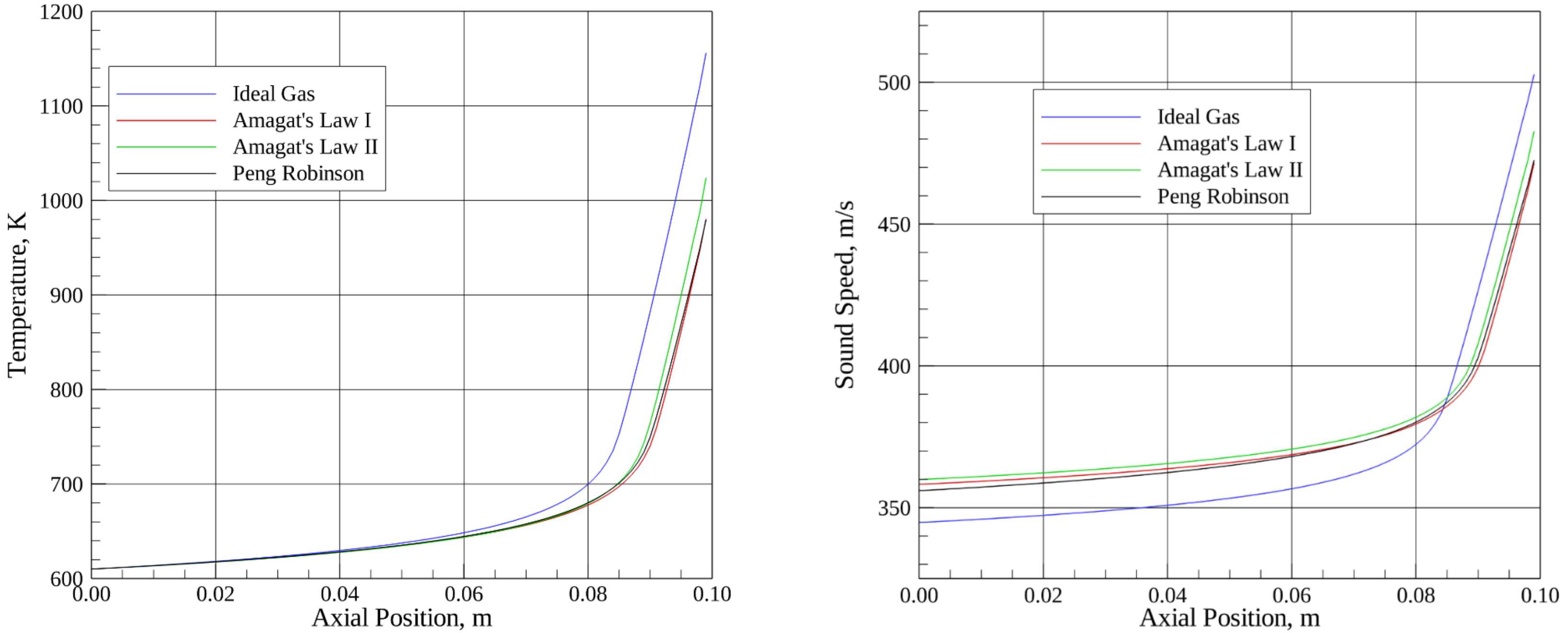

Ideal gas has a larger temperature increase compared to the real gas models.

Non-premixed Combustion

- Challenging demonstration
- The configuration is not numerically stable for the Peng-Robinson model
- 250,000 cell mesh, 2D simple injector
- $C_{12}H_{26}$ @ 600 K
- O_2 @ 610 K
- The initial pressure is 3.8 MPa
- Constant Z and Amagat's Law with real species was tested

Non-premixed Combustion

- With the constant compressibility model we observer a large amount of fluctuation in the density of the incoming $C_{12}H_{26}$
- This fluctuation is not seen in the real gas computation
- The shape of the density curve is fundamentally different for the two models and the constant compressibility is more likely to fluctuate

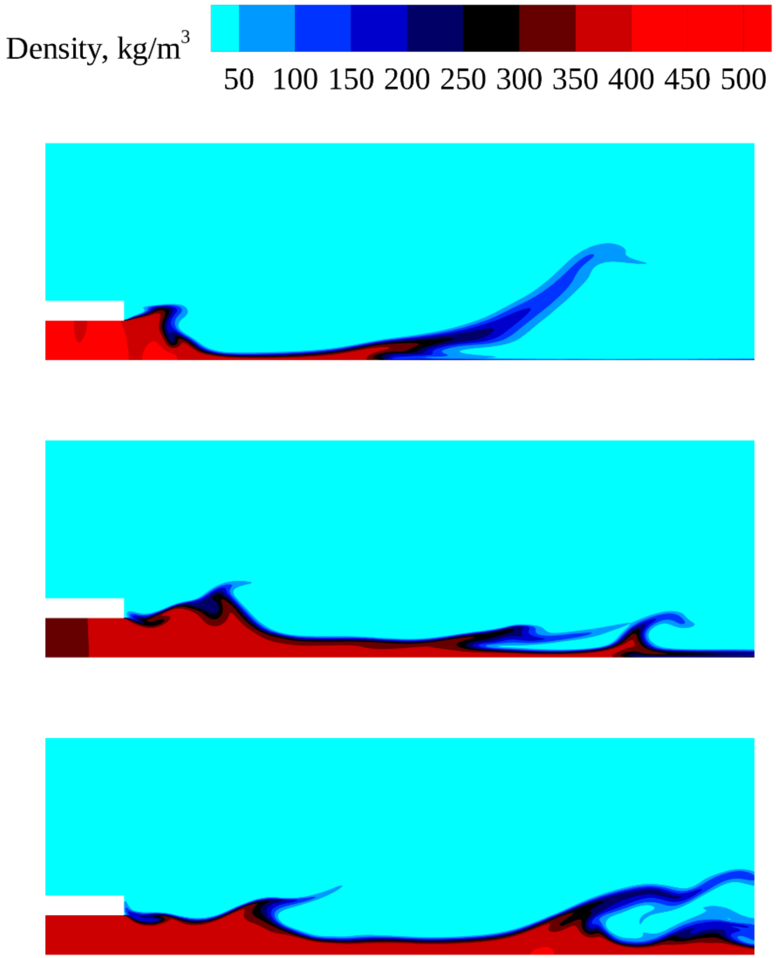

Non-premixed Combustion

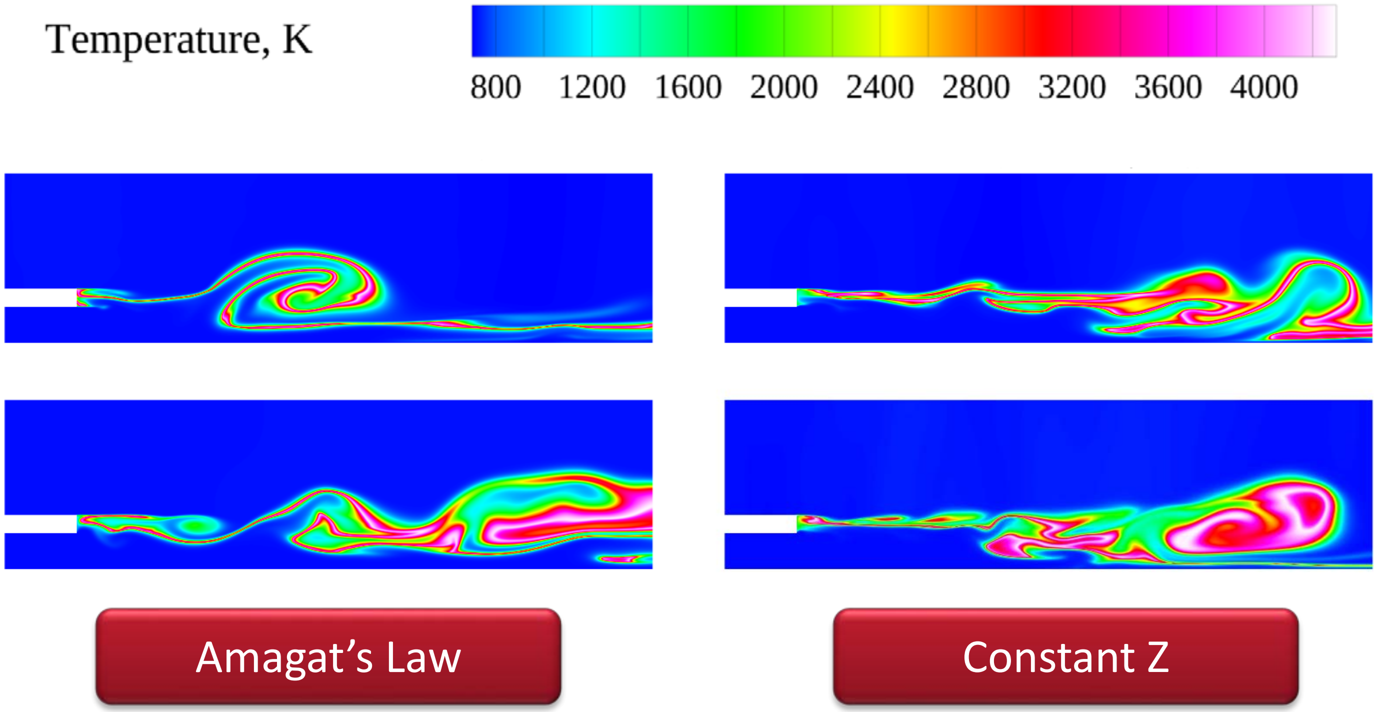

- Steeper gradients are present when using Amagat’s law, thinner flame features, impact on mixing in 3D?
- Both cases show an attached flame

Non-premixed Combustion

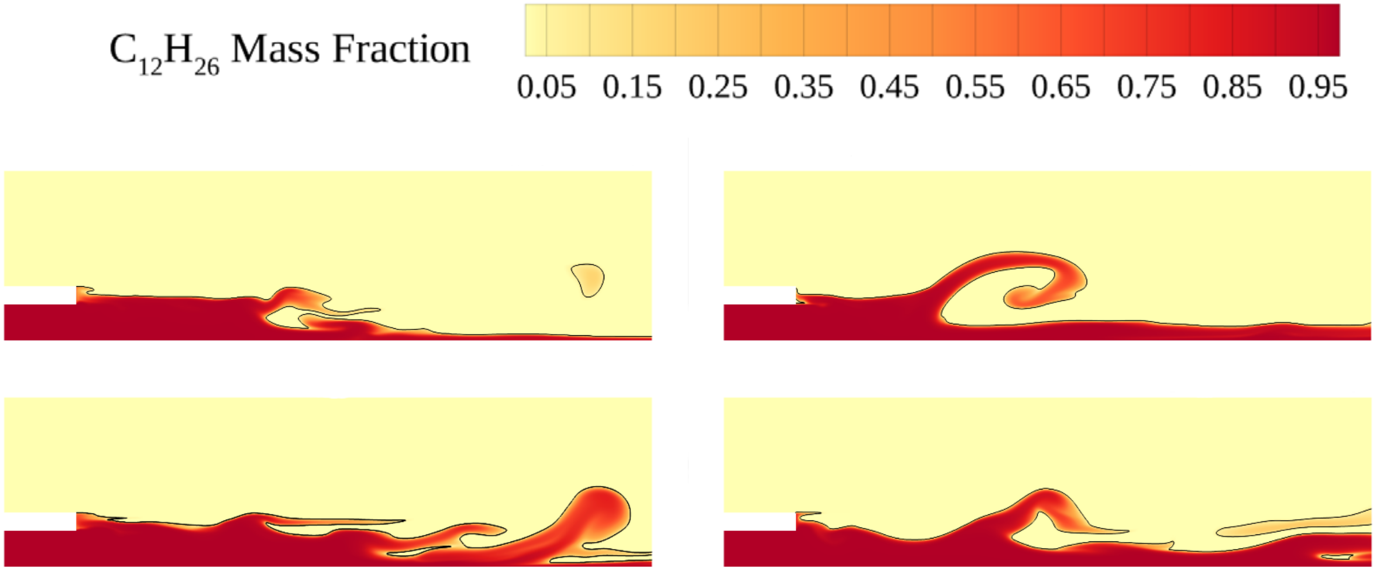

Amagat’s Law

Constant Z

- Steeper gradients are present when using Amagat’s law, thinner flame features, impact on mixing in 3D?
- Both cases show an attached flame

Summary

- Alternate approaches preserve some features of the complete real gas model, but not all
  - Numerical stability is improved but not solved
- Fundamental questions remain for the community
  - Are cubic equations of state the correct approach for combustion?
- Improvements in numerical robustness are needed
  - Recent work out of Stanford shows some potential success